TABLE OF CONTENTS

“Characterization of mitochondrial dysfunction in neural cell model of Parkinson’s disease”

The main focus of the project is the characterization of mitochondrial dysfunction in neural cell models of Parkinson’s disease (PD).

The first purpose was to investigate how Rotenone, a known neurotoxin, and H2O2, a known cytotoxic oxidant, reproduce a PD-related cell damage. Using MTT and Neutral Red viability assays, was then observed how these substances modulate cell death.

Secondary how mitochondrial impairment influences mitochondrial associated proteins, DJ-1 and Nrf2, linked to the pathophysiology of PD. Loss of DJ-1 is recruited by mitochondria under conditions of oxidative stress and can influence the translocation of Nrf2 to the nucleus to activate the antioxidant response element. Defects in DJ-1 have been identified in some familial forms of Parkinson’s disease and impairment of the antioxidant response is strongly linked to idiopathic cases. The effect of specific PD-related neurotoxins mitochondrial associated proteins was studied using SDS-PAGE gel electrophoresis and Western blotting.

At last the project was extended to investigate the molecular events that occur during mitochondrial dysfunction and whether this phenomenon can be modulated to maintain neuronal cell survival. In particular it has been analysed how the growth factors produced by Glioma cells culture could module the neuronal viability, in normal growth conditions and in neurotoxic conditions. The role that these factors may play in maintaining glial cell function is also of interest since these cells provide significant support to the dopaminergic neurones that are targeted in Parkinson’s disease.

1. INTRODUCTION

1.1 Parkinson's disease

Parkinson's disease (PD) is the second most common neurodegenerative disorder of the aging brain after Alzheimer's disease. It is a progressive neurological movement disorder characterized by the selective degeneration of dopaminergic neurons, mainly in the Substantia Nigra pars compacta, and the presence of proteinaceous intraneural inclusions known as Lewy bodies (Dauer et al., 2003).

The death of nigral dopaminergic neuron leads to a loss of the neurotransmitter dopamine in the striatum and consequent dysregulation of basal ganglia circuitries accounting for motor symptoms of PD such as resting tremor, slowness of voluntary movements, progressive rigidity and postural instability (Hardy at al.,2006).

Lewy bodies are spherical eosinophilic cytoplasmic aggregates composed of a variety of proteins including α-synuclein, ubiquitin, molecular chaperones and neurofilaments (Lees at al., 2009). These deposits are associated with non-motor features of PD such as autonomic dysfunctions, sleep disturbances, depression and cognitive impairments (Braak et at., 2005).

Current treatments, involving maintenance of dopamine levels, alleviate the motor dysfunction symptoms but do not prevent neurodegeneration due to the fact that researches are still unclear on the exact pathways directly causing neuronal cell death (Dawson et al., 2010).

The lack of a treatment for PD is the main motivation to study possible molecular mechanisms and to discover the exact pathophysiology of the disease. Several hypothesis have been proposed including mitochondrial dysfunctions, protein degradation impairment, neuroinflammation, oxidative stress, calcium homeostasis defects, lysosomal alterations and excitotoxicity (Navarro and Boveris, 2009). Although these features are linked, abnormal protein aggregation and mitochondrial dysfunctions due to the increase in oxidative stress are believed to primarily compromise neuronal survival (Nicholls and Budd, 2000).

1.2 Function and dysfunction of Mitochondria

Mitochondria are membrane-enclosed organelles which contain genetic material independent of nuclear DNA. These organelles produce most of the cell energy in the form of ATP along with their roles in signalling, cellular differentiation, cell growth and cell death.

The structure of a mitochondrion includes outer and inner membranes, intermembrane space and internal matrix. The inner membrane consists of the electron transport system complex, the ATP synthetase complex and transport proteins so as to be the site of energy production through oxidative phosphorylation. Depending on this process there are five intermembrane complexes (Complex I, II, III, IV, V) and two mobile electron carriers (Coenzyme Q and Cytocrome c).

As these organelles are one of the main sources of reactive oxygen species (ROS), they can themselves be affected by oxidative damage which can also turn into an apoptotic mechanism, the process of programmed cell death (Hwang, 2013). Many apoptotic responses occur in mitochondria such as the altered electron transport, the loss of membrane potential, the release of Caspase regulators, the attendance of pro- and anti- apoptotic family proteins. Therefore, it is plausible that the effect of mitochondrial dysfunctions can play a role in aging processes and degenerative diseases as PD (Lin et al., 2009).

1.3 Mitochondrial dynamics in PD

The direct relationship between mitochondrial dysfunction and PD comes from the post-mortem description of the Complex I deficit in the Substantia Nigra of patients with PD. In a study performed by Schapira et al. in 1990, the structure and the function of mitochondrial respiratory-chain enzyme proteins were analysed post-mortem in the substantia nigra of patients with Parkinson's disease. Total protein and mitochondrial mass of the PD patients were similar to the controls, whereas NADH-ubiquinone reductase (Complex I) and NADH cytochrome c reductase activities were significantly reduced.

Following studies identified a similar Complex I reduction in blood platelets, lymphocytes, muscle tissue and frontal cortex from PD patients. (Krige et al., 1992. Barroso et al., 1993. Penn et al., 1995.) However, it appears that the Substantia Nigra is more vulnerable to impairments of Complex I activity than the other regions and peripheral organs. In fact the increased levels of ROS generated within Dopamine neurons, as a result of Dopamine metabolism, lead to increased intracellular oxidative stress and reduced ATP production (Chinta and Andersen, 2008).

Complex I (NADH-quinone oxidoreductase) is one of the "entry enzymes" of cellular respiration. It is located in the inner mitochondrial membrane and it catalyses the transfer of electrons from NADH to Coenzyme Q10 (Ubiquinone). During both forward and reverse electron transfer, Complex I is a potential source of toxic ROS like superoxide and hydrogen peroxide. In particular, Superoxide contributes the most to cellular oxidative stress and cell death and it is thus linked to neuromuscular diseases and aging.

As oxidative stress and alterations in levels of antioxidants have been linked to the neurodegeneration, this has lent more evidence to the role of mitochondrial dysfunctions in PD (Dauer et al., 2003). Consistent with the systemic low-grade Complex I activity associated with PD, the second observation of Schapira et al. in 1990 was that this biochemical Complex I defection was the same as the one produced in animal models of parkinsonism by 1-methyl-4-phenyl-1,2,3,6-tetrahydropyridine (MPTP). Further support to the proposition that Parkinson's disease could be due to an environmental toxin with action similar to MPTP was given by Betarbet et al. in 2000, studying the effect of rats exposure to Rotenone.

Rotenone is a natural compound extracted from tropical plants and used as a pesticide that binds to the Ubiquinone binding site of Complex I and leaks electrons causing oxidative damage and cell toxicity (Kurshnareva et al. 2002). Afterwards chronic Rotenone treatments to rats result in

neuropathological and behavioural changes similar to human PD, including selective nigrostriatal degeneration and α-synuclein deposits (Sherer et al., 2003). Therefore chronic Complex I inhibition lead to destruction of substantia nigra par compacta neuron processes, morphologic changes, neural loss and decreased tyrosine hydroxylase protein levels in rodent postnatal midbrains (Testa et al., 2005).

1.4 PD-related genes and proteins

Most cases of PD are sporadic but there is a number of rare instances where PD is familial. Recent studies indicate that several PD-related genes, directly or indirectly, influence mitochondrial integrity providing a specific link to the mitochondrial dysfunctions observed in sporadic PD cases. (Hardy et al., 2006) The protein products of PD-associated genes include the E3 ubiquitin ligase Parkin, the PTEN-induced kinase 1 (PINK1), the redox-regulated chaperone DJ-1, the Leucine-rich Repeat Kinase 2 (LRRK2), the ubiquitin C-terminal hydrolase L1 (UCH-L1) and the presynaptic protein α-synuclein (SNCA).

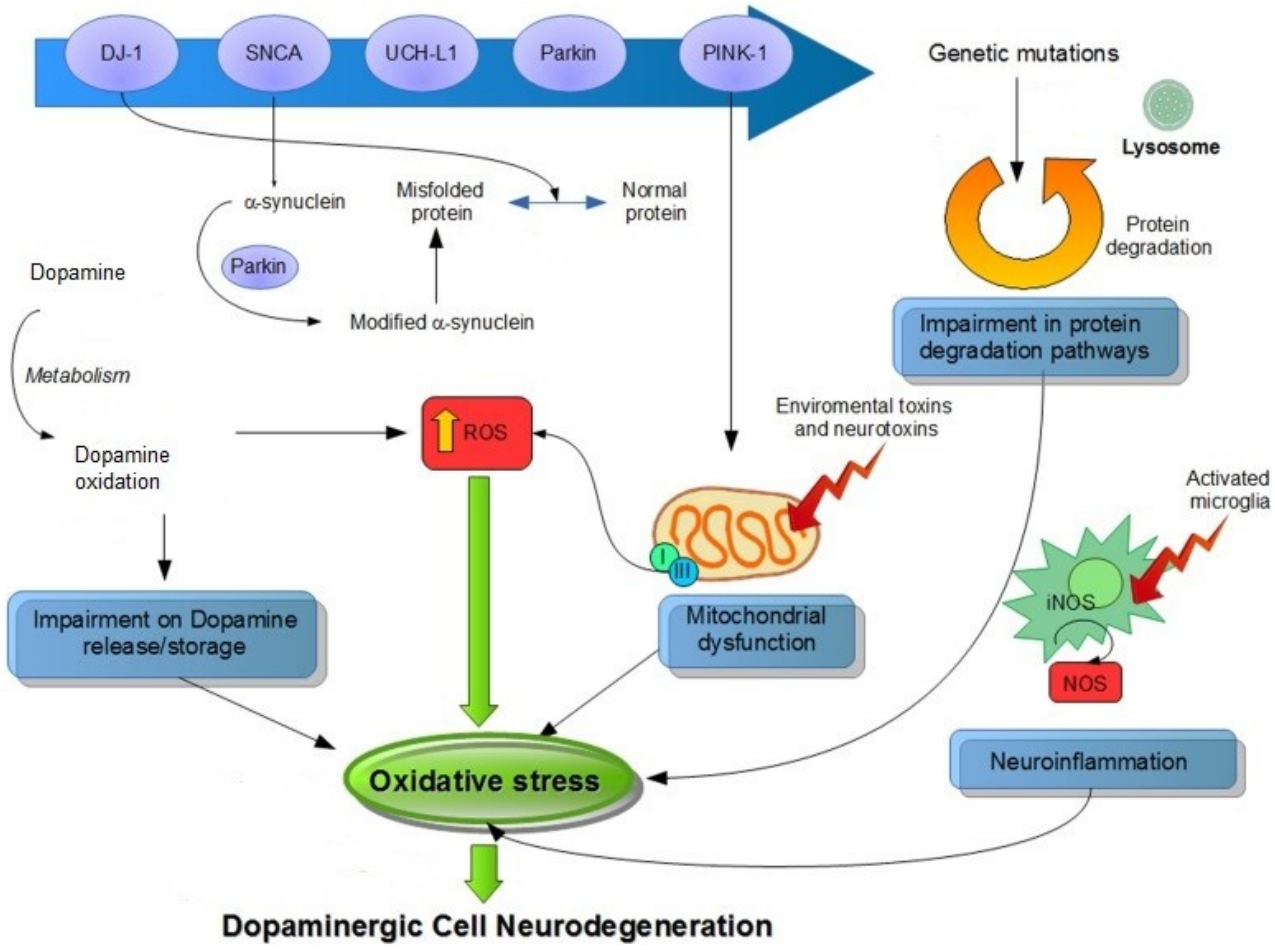

Figure : PD-related proteins pattern (Blesa et al., 2015)

The characterization of these genes again demonstrates the causal involvement of mitochondrial impairment and oxidative stress in PD pathogenesis, as several of them carry out important functions within mitochondria and act to reduce intracellular oxidative stress (Bonifatti et al., 2003).

Functional studies in cellular and animal models have shown that Parkin, PINK1 and DJ-1 mutations are primary cause of early autosomal recessive forms of PD (Fitzgerald and Plun-Favreau, 2008). They are part of a pathway that is involved in maintaining the mitochondrial integrity within certain tissue, including dopaminergic neurons in the brain. They seem to work together to help maintain mitochondrial homeostasis but their mechanism and their relationship still remain unclear.

1.5 PINK1

PTEN-induced kinase 1 is a serine/threonine kinase mainly localized in mitochondrial environment and present in the cytoplasm under the influence of particular cell conditions. The action of this kinase is required for mitochondrial protection as it prevents oxidative stress-induced release of cytochrome c and consequent apoptosis (Bueler, 2009).

In fact PINK1 phosphorylates two proteins localized in the mitochondrial intermembrane space, TRAP1 (TNF-receptor-associated protein 1) and HtrA2/Omi. Phospho-TRAP1 inhibits cytochrome c release and then acts as a chaperon to prevent misfolding or promote assembly of mitochondrial proteins under oxidative stress conditions (Pridgeon et al., 20017. Plun-Favreau et al., 2007).

1.6 Parkin

Parkin is a cytosolic E3 ubiquitin-protein ligase that promotes the degradation of unfolded or impaired proteins by the proteasome system. An increase of oxidative stress, that induces mitochondrial malfunction, triggers a rapid and specific translocation of the cytosolic Parkin to the mitochondria which manifest a reduced membrane potential (Shimura et al., 2000).

Within the mitochondrion, Parkin promotes Mytophagy, the lysosome degradation process of damaged mitochondria (Bueler, 2009). Furthermore Parkin acts as a potent cell protector factor inhibiting the cytochrome c release and suppressing pro-apoptotic effectors that lead to caspase activation and cell death by apoptosis (Darios et al., 2003. Kuroda et al.,2006).

Parkin effects are facilitated by the cytosolic PINK1 phosphorylation that triggers its translocation from the cytosol into the mitochondrion. However this phosphorylation is not essential as Parkin activity has been found unchanged in PINK1-deficient cells (Kim et al., 2008).

1.7 DJ-1

DJ-1 was first linked to PD when deletion mutations in its gene were discovered to cause a familial early form of the disease (Bonifati et al., 2003). In fact DJ-1 is an oxidative stress-regulated chaperone and transcriptional modulator that shifts from the cytosol to mitochondria and to the nucleus upon oxidation of specific cysteine residues (Canet-Aviles et al.,2004).

Under basal condition it is present mostly in the cytosol, but under oxidative stress conditions it redistributes to mitochondria and later to the nucleus correlating the ability of DJ-1 to confer neuroprotection (Junn et al.,2009). DJ-1 mitochondrial translocation starts with the oxidation of the cysteine residue 106, to the cysteine-sulfinate and then cysteine-sulfonate, which is probably facilitated by binding to other mitochondrial chaperons (Li et al.,2005). Because of these characteristics, DJ-1 thus possesses quenching activity against ROS by self-oxidation of its cysteine residues (Taira et al.,2004).

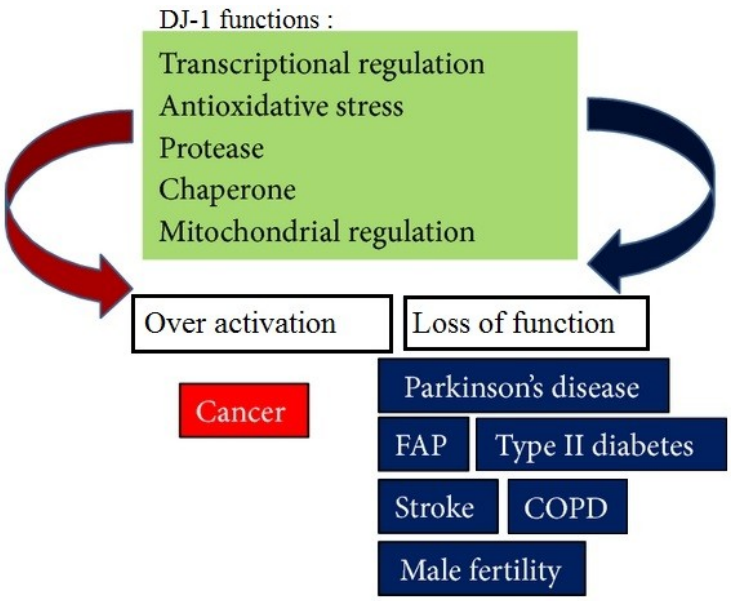

Figure : DJ-1 functions and its related diseases (Ariga et al, 2013).

As a chaperon DJ-1 prevents the misfolding and the aggregation of oxidized mitochondrial proteins, like alpha-synuclein, suggesting a protective role against electron transport chain activity impairments. Moreover, loss of function or mutations of DJ-1 render animals and cultured cells more susceptible to oxidative stress and mitochondrial toxins, as Complex I inhibitors, implicated in sporadic PD. This suggests that other possible target of DJ-1 would be subunits of mitochondrial respiratory complexes and in particular of Complex I (Lev et al., 2007).

As a transcriptional modulator DJ-1 regulates the activity of DNA-binding transcription factors such as p53, Nuclear factor erythroid-2-related factor 2 (Nrf2), sterol regulatory element binding protein (SREBP), androgen receptor and polypyrimidine tract-binding protein-associated splicing factor (PSF).

1.8 Nrf2

Nrf2 is a transcription factor located within the cytosol of the cell and regulated by a cytosolic protein called Kelch-like ECH-associated protein 1 (Keap1). Keap1 binds Nrf2 and regulates it negatively by promoting its sequestration in the cytosol and its degradation. Unless Nrf2 is activated, it is ubiquitinated by the E3-ubiquitin ligase-like domain of Keap1 and degraded by proteasome. Signals of oxidative stress, as the presence of DJ-1 within the cytosol, induce the separation of Nfr2 from Keap1 and suddenly its translocation into the nucleus. Following its nuclear translocation, Nrf2 binds the antioxidant response elements (ARE) in the promoter region of its target genes (Tufekci et al., 2011) activating the antioxidant defence system and mitochondrial biogenesis.

The Nrf2-ARE pathway is thus a signaling pathway responsible for controlling the expression of genes that are involved in eliminating oxidative products, such as NADPH quinone oxidoreductase-1 (NQO-1) and electrophilic agents that increase the cell antioxidant capacity. In cases of PD and other neurodegenerative disorders, the activation of this pathway causes a potential neuroprotective response (Nguyen et al., 2009).

The interaction of Nrf2 with the parkinsonian protein DJ-1 may provide another link between Nrf2 function and PD. Upon oxidative stress, the transcriptional modulation activity of DJ-1 allows to stabilize Nrf2 by preventing its interaction with Keap1 and its consequently degradation leading to the translocation of Nrf2 into the nucleus (Clements et al., 2006).

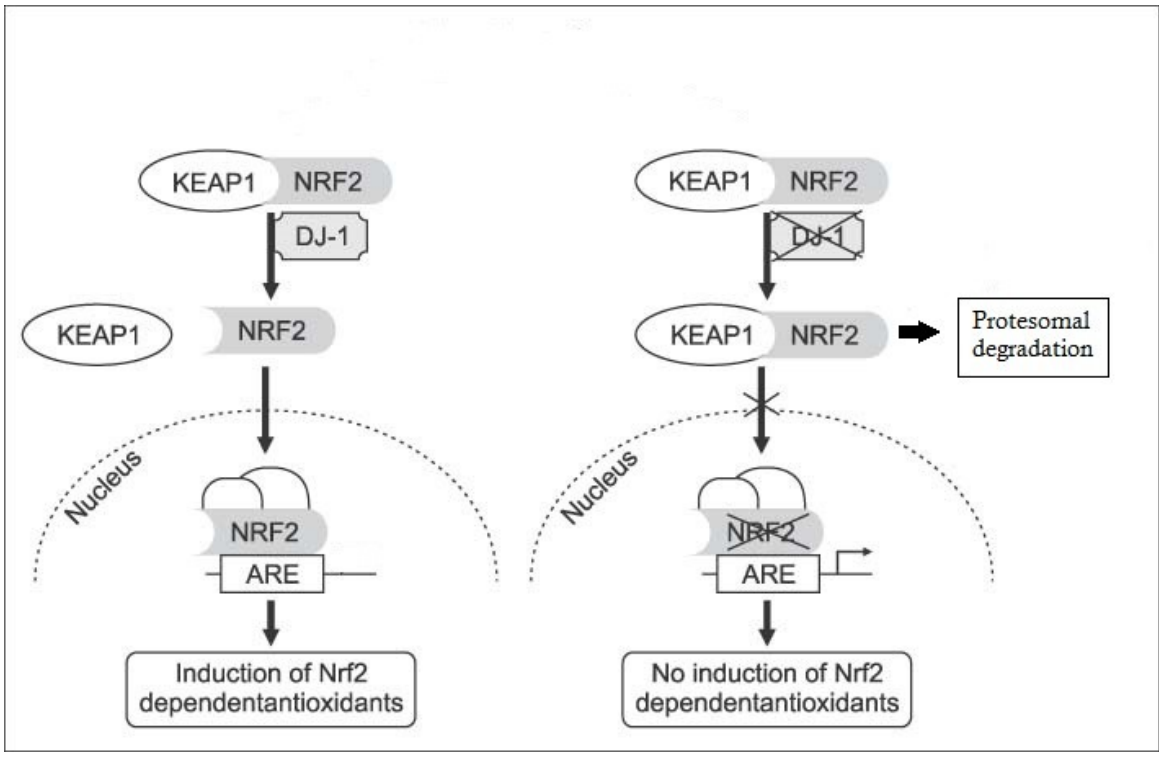

Figure 3 : Nrf2 activation by DJ-1 (Lee et al., 2009)

It was first believed that when Nrf2 was activated by cellular signals in times of stress, it would break from Keap1 and translocate from the cytosol into the nucleus. However, it has been discovered that due to Nrf2's unstable nature, it can also translocate into the nucleus during times of non-stress within the cell in order to receive stability (Nguyen at al., 2009).

Further understanding of the functions of the mentioned target mitochondrial proteins, DJ-1 in particular, has the potential to provide insight on the pathogenesis of PD. For this investigation, we set out to continue to investigate how DJ-1 is impaired in PD-related conditions by exposing the human neuroblastoma cell line SH-SY5Y to a Rotenone-induced oxidative stress and measuring their viability. We also investigated the potential link between DJ-1's protection against neurotoxicity and the activation of the Nrf2-ARE pathway, ultimately leading to a neuroprotective response.

1.9 Glia's neuroprotective role in PD

The last purpose of our study was to investigate how glial neurotrophic products promote proliferation and neuroprotection by exposing the cell line SH-SY5Y to rotenone and to a medium from a culture of the human glioblastoma cell line U-87 MG.

Neuroglia provides support and protection for neurons in both central nervous system and peripheral nervous system. Glia's main functions are to facilitate the development and plasticity of the nervous system, to regulate the fluid surrounding neurons and their synapse, to supply nourishment and oxygen to neurons, to destroy pathogens and remove dead neurons.

In particular astrocytes, the most abundant type of macroglial cells in central nervous system, have numerous projections that link neurons to their blood supply while forming the blood-brain barrier. Furthermore, they regulate the external neural environment by removing excess of potassium ions and recycling the neurotransmitters during synaptic transmission. Astrocytes produce various substances, primarily ATP which is used to communicate with each other by gap junctions ("Studying the Nervous Systems of Humans and Other Animals" Purves et al., 2004).

A study performed by Larsen et al. in 2011 demonstrated that knockdown and knockout of DJ-1 expression in astrocytes impairs astrocyte-mediated neuroprotection against oxidative stress. Therefore a recent study of Dukhande et al. in 2013 demonstrated that a co-culture of a human glioblastoma U-87 cell line could protect a neuroblastoma SK-N-SH cell line against mitochondrial dysfunction and apoptotic death induced by depletion of mitochondrial glutathione (GSH). Consequently, neuroprotective factor are secreted by astrocytes and are indeed potential candidates for rescuing neurons under oxidative stress and degeneration such as Parkinson's disease.

2. MATERIALS AND METHODS

2.1 Cell Cultures

Human neuroblastoma SH-SY5Y cells were cultured in a media containing 90% Dulbecco's Modified Eagle's Medium Ham's F-12 (DMEM) enriched with 2mM L-Glutamine, 10% heat inactivated Fetal Bovine Serum, 1% penicillin/streptomycin and 1% non-essential amminoacids.

Human Glioblastoma Astrocytoma U-87 MG cells were cultured in Eagle's Minimum Essential Medium (EMEM) supplemented with 2mM L-Glutamine, 10% heat inactivated Fetal Bovine Serum, 1% penicillin/streptomycin and 1% non-essential amminoacids.

Cells were maintained as monolayer under sterile conditions in a 25 cm^2 surface area/10 ml volume (T-25) flask. They were cultured in an incubator with 95%air and 5% CO_2 humidified atmosphere at 37°C. The morphology of the cells was recorded using a camera (Primovert HDcam) attached to an inverted light microscope (Primovert, ZEISS).

2.2 Trypsinization and Cell Count

Medium was aspirated from T-25 flask and the attached monolayer of SH-SY5Y cells were gently washed twice in phosphate buffered saline (PBS). Then cells were exposed to 1X trypsin in an incubator at 37°C for 5 minutes. Detached cells were then suspended in fresh medium and placed in a centrifuge (MIRKO 200) for 5 minutes at 300rpm. Resulting cell pellet was re-suspended in a 1:10 dilution of medium and counted using a haemocytometer under a microscope.

2.3 Cell Treatments

Cell viability under oxidative stress conditions was determined by placing 5000 cells of SH-SY5Y in each well of the half of two 96-wells plates and were then allowed to grow for 48 hours. Half of the first plate was treated with rotenone at the concentrations of 0, 0.1, 0.5, 2.5 and 10 µM. Half of the second plate was treated with hydrogen peroxide (H2O2) at the concentration of 0, 100, 200, 500, 1000 and 2000 µM. Both plates were then incubated at 37°C, the rotenone for 48 hours and the H2O2 for 24 hours.

Cell viability in presence of potential neuroprotective factors and oxidative stress conditions, was determined by placing 2500 SH-SY5Y cells in each well of a 96-well microplate that were allowed to grow for 48-72 hours. Then half plate medium was aspirated and replaced with a mixture of DMEM and EMEM media (1:1) and Rotenone at the concentrations of 0, 0.1, 0.5, 2.5 and 10 µM. The medium of the other half-side of the plate was aspirated and replaced with the previous rotenone concentrations and a mixture of DMEM and GLIOMA media (1:1). This glioma medium was formerly collected from a human glioblastoma astrocytoma U-87 MG culture, centrifuged and stored at 4°C.

Cell proliferation in presence of different media was measured in both 96-well plates and T-25 flask culture environments, by separately placing SH-SY5Y cells with DMEM medium as a control, with a mixture of DMEM-EMEM and a mixture of DMEM-Glioblastoma cultured medium. The cells were incubated in T-25 flask for 2 and 3 days, while 5000 cells were plated in each well of a 96-wells plate and incubated for 1, 2 and 3 days.

2.4 Cell Viability: MTT Assay

Cell viability was primarily monitored by measuring cellular mitochondrial activity. At the end of each treatment, 10ul of MTT (3-(4,5-dimethylthiazol-2-yl)-2,5-diphenyltetrazoulium bromide) were added to each well and then incubated for 1 hour at 37°C. The culture medium was aspirated from each well and then the resulting product was solubilized in 100 µl dimethyl sulfoxide (DMSO). After agitating for 2 minutes on a plate shaker, the absorbance for each plate was taken at 570nm in a plate reader (UVM 340 plate reader and Harrier 15/80 Omega BMG Labtech microplate reader). Same methods but different solutions volumes, were used to measure the viability of the cell suspension extracted from T-25 flask.

2.5 Cell Viability: Neutral red Assay

Cell viability was determined also by measuring cellular lysosomal activity. At the end of the treatment, the cultured medium was removed from each well, replaced with 100ul of Red Medium (1:10 dilution of Neutral Red solution 40mg/10ml in growth medium) and incubated for 2 hours at 37°C. The Red medium was then carefully aspirated from each well and the resulting product was solubilized in 100 µl of Red Solution (made with 50% Ethanol, 49% deionised water and 1% glacial acetic acid). After agitating for 10 minutes on a plate shaker, the absorbance for each plate was read at 540 nm in UVM 340 plate reader and Harrier 15/80 Omega BMG Labtech microplate reader.

2.6 Protein Estimation

The samples for protein estimation were performed by an incubation of four T-25 flasks containing SH-SY5Y cells for 72 hours in a 37°C humidified atmosphere, followed by a treatment with Rotenone at 0, 0.1, 0.5, 2.5uM concentrations for 48 hours. Cells were then collected from each flask by using a cell scrapper and spun down by a centrifuge at 300rpm for 5 minutes. Once collected, the resulting cell pellets were washed twice with 1ml of PBS and spun a final time in a microfuge MIKRO 200 at 10,000rpm for 5 minutes. Triplicates of protein standards were prepared using bovine serum albumin (BSA), RIPA extraction buffer and distilled water. SH-SY5Y cell samples Rotenone treated were prepared by adding 250ul of RIPA buffer, containing phosphate inhibitor, to each sample and then mixed using a Whirlimixer for 1 minute. Samples were then spun in the microfuge at 14,000rpm for 10 minutes and 10ul of each sample resulting supernatant was added to 90ul of distilled water.

According to the Lowry method, 1ml of Lowry reagent (96.3% sodium carbonate/sodium hydroxide solution, 1% (w/v) copper sulphate solution, and 2.7% (w/v) NaK-tartrate solution) was added to each sample and allowed to incubate at room temperature for 15 minutes. 100ul of diluted Folin-Ciocalteau (diluted 1:1 with distilled water) was added to each tube, vortexed mixed, and incubated for 30 minutes at room temperature.

100ul of each sample (standards and cell samples) were plated out into a 96-well plate and the absorbance was read at 750nm using a POLAR star Omega plate reader. Calibration curve was then created using Microsoft Excel and estimated protein concentration of each unknown cell sample was measured using the curve as a standard.

2.7 SDS-PAGE and semi-dry Western Blotting

Protein samples were prepared using calculated volumes from protein estimation (section 2.6) in order to contain 15ug of protein and equally matched in volume of 2x Laemmli running buffer. Samples were then heated in a Techne Hot Block at 100°C for 5 minutes. A protein standard was loaded into the stacking gel of a 12% polyacrylamide Mini-PROTEAN TGX Precast Gels (Bio-RAD) along with the heated protein samples, then the gel was ran at 150V for 1 hour.

Proteins separated by sodium dodecyl sulphate polyacrylamide gel electrophoresis (SDS-PAGE) were transferred onto a nitrocellulose membrane by a Semi-Dry Western Blotting. Using a transfer buffer (48mM Tris, 39mM glycine, 0.0375% SDS, and 20% methanol) to soak the transfer filter paper and the nitrocellulose, a filter paper sandwich formed of the gel and the membrane was created on a Western Blot transferring block and the protein gel was transferred to the nitrocellulose paper by allowing it to run in the block for 1 hour at 50mA.

2.8 Copper Stain

Blotting efficiency was checked by staining with a reversible copper stain (copper phthalocyanine 3,4',4',,4''' tetrasulphonic acid tetrasodium salt). Nitrocellulose membrane was immersed in copper stain for 2-3 minutes with agitation and then rinsed using distilled water. Once protein bands were visible, nitrocellulose was cut as needed based on the size of the appropriate targeted proteins. De-staining of the copper stain was then achieved by performing multiple washes with drops of 4M NaOH in distilled water until the blue stain was completely removed.

2.9 Immunoprobing

The immunoprobing of the targeted DJ-1 and NRF-2 proteins was achieved by a previous incubation of the nitrocellulose membranes in a blocking solution, made up of 3% (w/v) Marvel milk powder diluted in tris buffer saline (TBS) at pH 7.4 and 0.1% Tween20, at room temperature for one hour while using a plate shaker. Blocked membranes were then rinsed with distilled water and incubated with primary antibodies (anti-DJ-1 and anti-Nrf2 rabbit antibodies) in a 3% BSA

solution overnight at 4°C. Unbound primary antibodies were removed by shaking in a TBS 1X-Tween20 solution for 10 minutes and repeating the wash five times. Nitrocellulose membrane was then incubated with an alkaline phosphate conjugated-secondary antibody solution (anti-IgG rabbit antibodies diluted 1:100 in 3% Marvel milk and TBS-Tween) for two hours at room temperature while shaking. Blots were finally washed five times in TBS-Tween and rinsed in distilled water for 2 minutes at room temperature.

2.10 Alkaline Phosphate Detection

The protein bands on the nitrocellulose paper were detected by using a substrate buffer of 0.75M Tris at pH 9.5 containing 0.13mM of Nitro Blue tetrazolim (NBT) and 0.29mM 5-bromo-4-chloro-3-indolyl phosphate (BCIP). Substrate buffer solution was poured over nitrocellulose, covered and placed on a plate shaker. Formation of bands was checked at 5 minute intervals and the resulting bands were read in a Bio Rad ChemiDoc MP imaging system.

2.11 Statistical Analysis

All data is expressed as the means of each replicated or triplicated experiment. The statistical significance of the data was tested by Student's t-test for single comparisons. p value < 0.05 was considered statistically significant for each case. All statistical analyses tests were performed using Microsoft Excel 2010.

3. RESULTS

3.1 Effects of mitochondrial impairment and oxidative stress on SH-SY5Y cells.

In order to reproduce a neural cell model of PD, human neuroblastoma SH-SY5Y cell line was treated with multiple concentrations of Rotenone, a known mitochondrial Complex I inhibitor. Alongside the Rotenone tests, treatments with H2O2, a common known oxidant, were performed in order to compare the effects on cell viability between the two compounds. Rotenone concentrations used were 0.1uM, 0.5uM, 2.5uM, 10uM and 0uM as the control. H2O2 concentrations were 100uM, 200uM, 500uM, 1000uM, 2000uM and 0uM as the control.

Both treatments onto the cells caused various responses including changes in the morphology of viable cells and cell shrinkage leading to possible apoptosis (Figures 4 and 5). As exhibited in Figures 4-D and 4-E, cell death occurred at the concentration of 2.5uM and 10uM Rotenone represented by a reduction in cell volume and a loss of the spherical cell shape. A similar cell morphology resulted at the concentration of 500uM and 1000uM H2O2 (Figures 5-D and 5- E), whereas 2000uM H2O2 (Figure 5-F) resulted only in a few rounded dead cells.

Suddenly the cell viability was detected by MTT and Neutral Red assays.

The MTT (3-(4,5-dimethylthiazol-2-yl)-2,5-diphenyltetrazolium bromide) tetrazolium reduction assay is based on the characteristic of viable cell with active metabolism to convert MTT into a purple coloured formazan product with an absorbance near 570nm. When cells die, they lose the ability to convert MTT into formazan, thus colour formation serves as a marker of only the viable cells. The formazan product accumulates as an insoluble precipitate inside cells that must be solubilized in DMSO prior to recording absorbance readings. The amount of signal generated is dependent on several parameters including: the concentration of MTT, the length of the incubation period, the number of viable cells and their and metabolic activity. All of these parameters should be considered when optimizing the assay conditions to generate a sufficient amount of product that can be detected above background. Thus the quantity of formazan, presumably proportional to the number of viable cells, is measured by recording changes in absorbance at 570nm using a plate reading spectrophotometer. The exact cellular mechanism of MTT reduction into formazan is not well understood, but likely involves reaction with NAD(P)H or similar reducing molecules that transfer electrons to MTT. However, speculation in the early literature involving specific mitochondrial NAD(P)H-dependent enzymes has led to the assumption that MTT measures mitochondrial activity (Riss et al., 2004-2013).

The Neutral Ned uptake assay is based on the ability of viable cells to incorporate and bind the neutral red dye in the lysosomes. This cationic dye penetrates cell membranes by passive diffusion and concentrates in the lysosomes, where it binds to anionic and phosphate groups of the lysosomal matrix by electrostatic hydrophobic bonds. At physiological pH the dye presents a net charge close to zero enabling it to penetrate the membranes of the cell, whereas inside the lysosomes, where a proton gradient maintains a low pH, the dye becomes charged and it is

retained. When the cell dies or the pH gradient is reduced, the dye is not retained. Consequently, the amount of retained dye is proportional to the number of viable cells. In addition, the uptake of neutral red by viable cells can be modified by alterations in cell surface or lysosomal membranes thus it is possible to distinguish between viable, damaged or dead cells. The neutral red dye is then extracted from the viable cells using an Ethanol solution and the absorbance of the solubilized dye is quantified using a spectrophotometer (Repetto et al., 2008). In conclusion intrinsic differences between the two assays allowed to measure cell viability comparing mitochondrial and lysosomal activity.

As shown in Figures 6 and 7, the percentage of cell viability of neuroblastoma cells by MTT assay decreased in each case, from 100% at the control to 10% at 2.5uM of Rotenone and to 6% at 1000uM of H2O2.

In Figures 8 and 9 is shown that the percent cell viability decreased also in each case obtained by the Neutral Red assay, from the 100% at the control to 57% at 2.5uM of Rotenone and to 21% at 1000uM of H2O2. Possible outliers are present between 2.5uM and 10uM of Rotenone, with a rise of 9%, and between 1000uM and 2000uM, with a rise of 10%.

Data collected were considered statistically significant by the use of a Student T-test, containing a p-value < 0.05. In MTT assay, 0.1uM of Rotenone and 100uM of H2O2 were determined to do not have a statistically significant drop in percent cell viability compared to the control, whereas 10uM of Rotenone and 2000uM of H2O2 did not have statistical importance compared to the previous respective treatment concentration. In Neutral Red assay, 100uM and 200uM H2O2, 0,1um and 0,5uM of rotenone were determined to do not have a statistically significant drop in percent cell viability compared to the control; whereas 10uM of Rotenone and 2000uM of H2O2 did not have statistical importance compared to the previous respective treatment concentration.

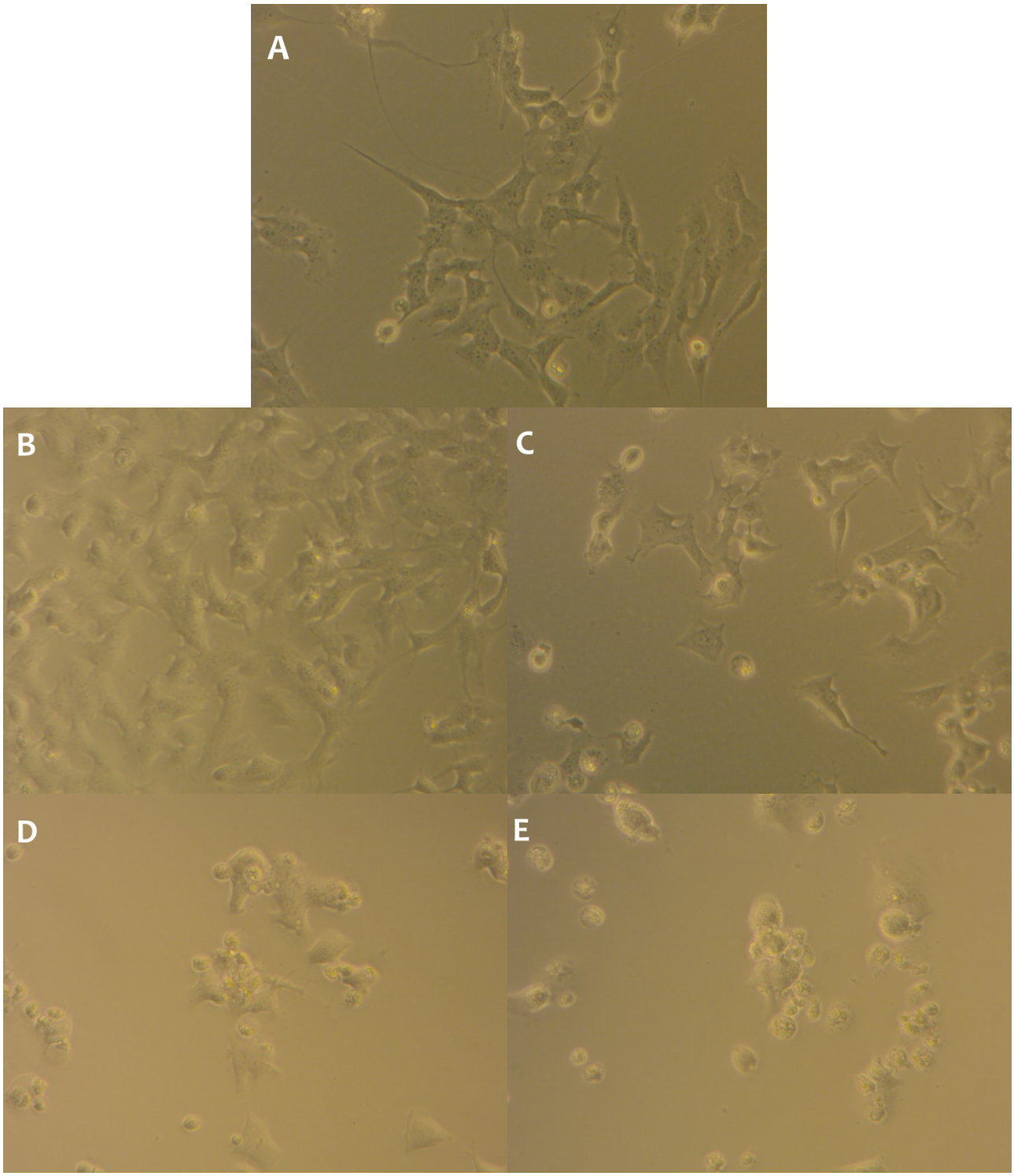

Figure 4 : Pictures of human neuroblastoma SH-SY5Y cells after 48 hours Rotenone treatment.
A) Un-treated neuronal cells used as the control; B) cells treated with 0.1uM of Rotenone showed a slight shrink on dendrites; C) cells treated with 0.5uM of Rotenone showed a decrease in cell size and some dead cells can be observed; D) cells treated with 2.5uM of Rotenone displayed a vast change in morphology alongside apoptosis; E) cells treated with 10uM of Rotenone displayed large apoptosis, most of the cells were dead. Images taken with a Zeiss model microscope using ZEN imaging software.

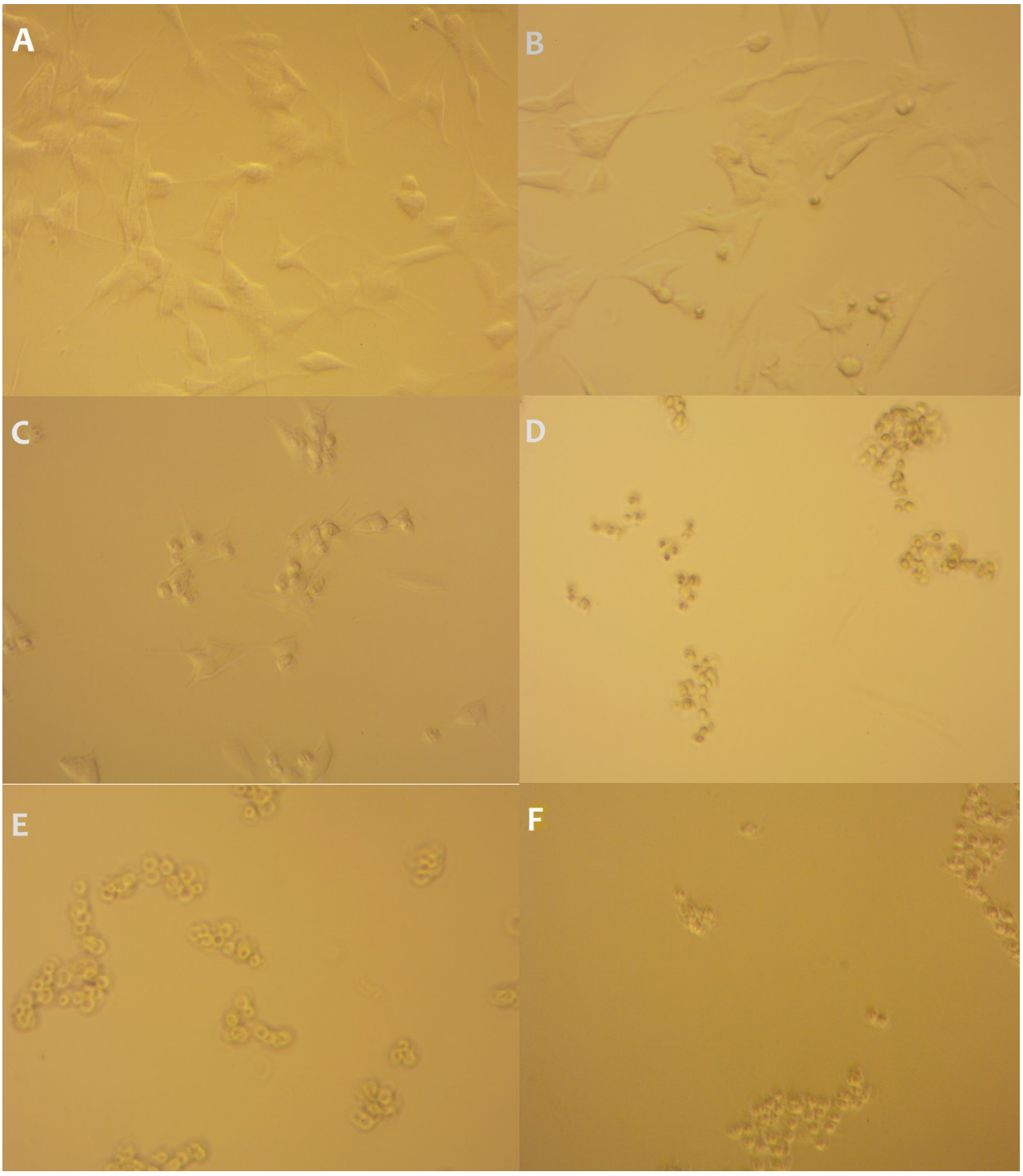

Figure 5 : Pictures of human neuroblastoma SH-SY5Y cells after 24 hours H2O2 treatment.
A) Un-treated neuronal cells used as the control; B) cells treated with 100uM of H2O2 showed a strong shrink in morphology and minimal cell death; C) cells treated with 200uM of H2O2 showed a vast drop in cell size and some dead cells can be observed; D) cells treated with 500uM of H2O2 displayed apoptosis; E) cells treated with 1000uM of H2O2 displayed apoptosis; F) cells treated with 2000uM of H2O2 showed large apoptosis, most of the cells were dead. Images taken with a Zeiss model microscope using ZEN imaging software.

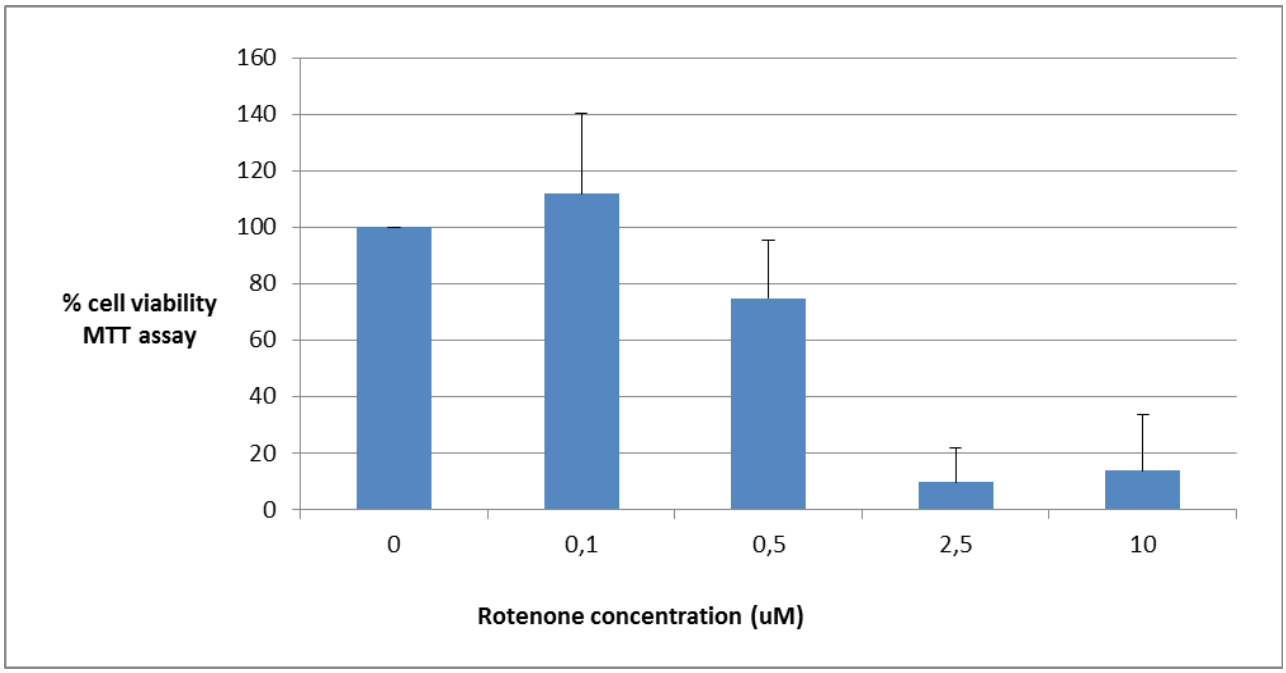

Figure 6 : Graphical representation of MTT viability assay performed on human neuroblastoma SH-SY5Y cell line after 48 hours treatment with multiple concentrations of rotenone. Data collected were considered statistically significant by the use of a Student T-test, containing a p-value < 0.05. 0.1uM was determined to do not have a statistically significant drop in percent cell viability compared to the control, whereas 10uM did not have statistical importance compared to the previous treatment.

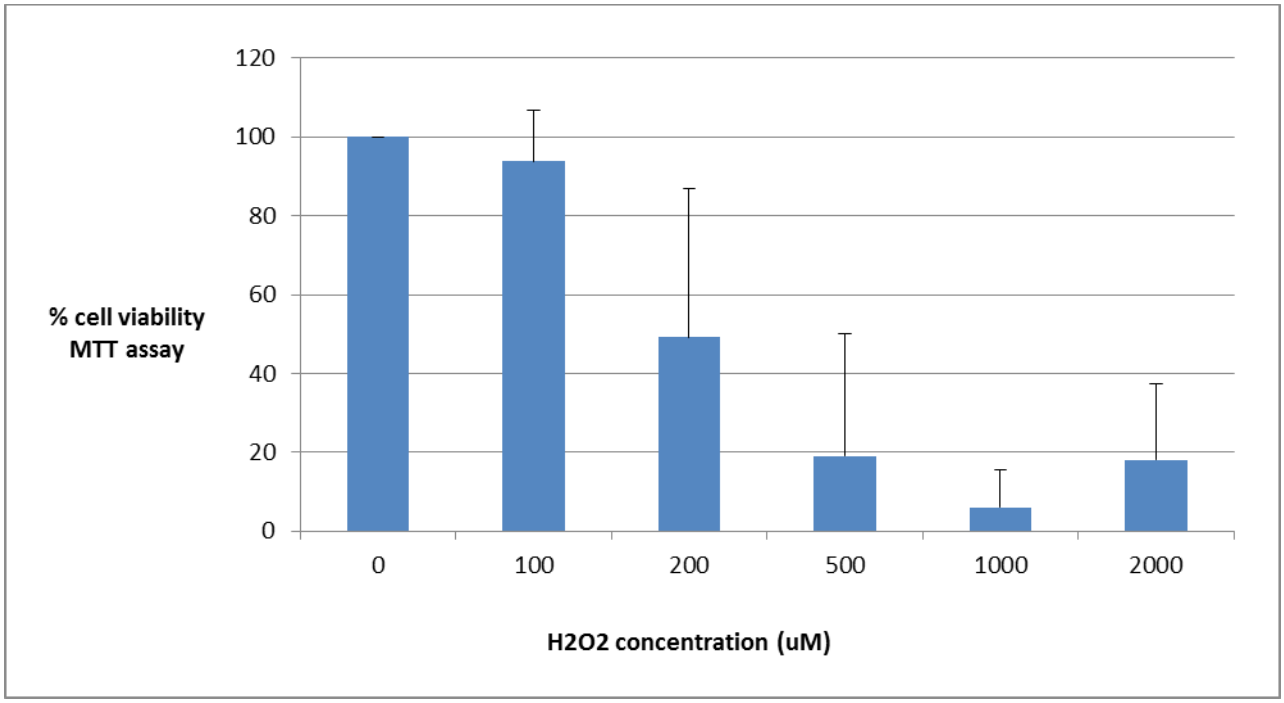

Figure 7 : Graphical representation of MTT viability assay performed on human neuroblastoma SH-SY5Y cell line after 24 hours treatment with multiple concentrations of Hydrogen peroxide. Data collected were considered statistically significant by the use of a Student T-test, containing a p-value < 0.05. 100uM was determined to do not have a statistically significant drop in percent cell viability compared to the control, whereas 2000uM did not have statistical importance compared to the previous treatment.

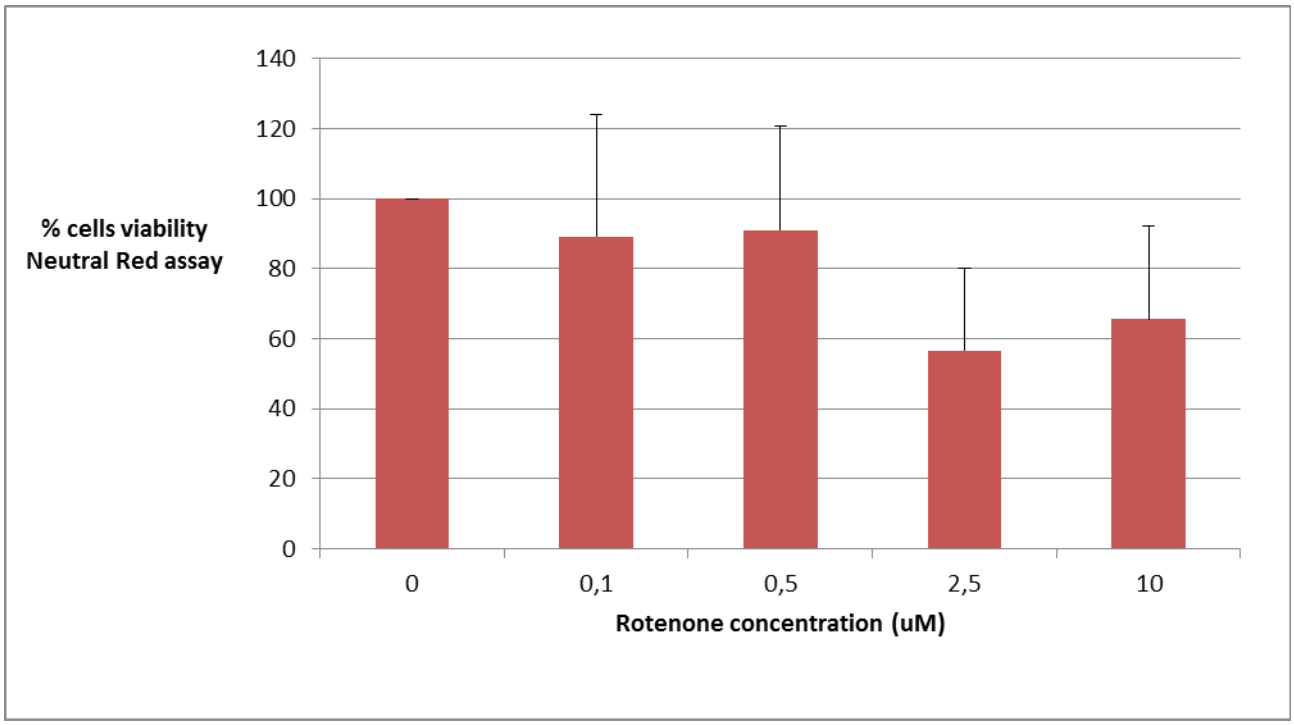

Figure 8 : Graphical representation of Neutral Red viability assay performed on human neuroblastoma SH-SY5Y cell line after 48 hours treatment with multiple concentrations of Rotenone. Data collected were considered statistically significant by the use of a Student T-test, containing a p-value < 0.05. 0,1 uM and 0,5uM were determined to do not have a statistically significant drop in percent cell viability compared to the control, whereas 10uM did not have statistical importance compared to the previous treatment.

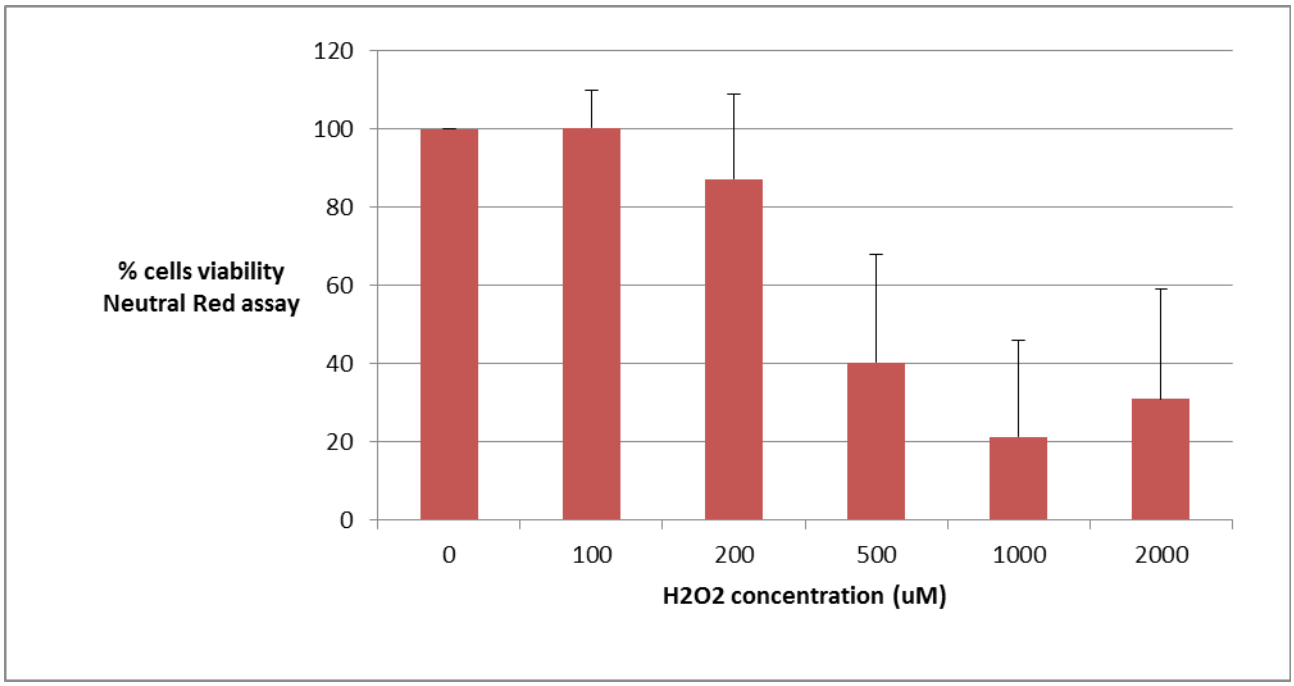

Figure 9 : Graphical representation of Neutral Red viability assay performed on human neuroblastoma SH-SY5Y cell line after 24 hours treatment with multiple concentrations of Hydrogen peroxide. Data collected were considered statistically significant by the use of a Student T-test, containing a p-value < 0.05. 100uM and 200uM were determined to do not have a statistically significant drop in percent cell viability compared to the control, whereas 2000uM did not have statistical importance compared to the previous treatment.

3.2. Possible Rotenone-induced modulation of DJ1 and Nrf2 proteins on SH-SY5Y.

In order to estimate the protein amount within Rotenone-treated SH-SY5Y cells pellet samples, protein estimation by Lowry Method was used as a precursor technique for SDS-PAGE gel and Western Blotting analyses. Thirteen known protein-containing solutions of BSA were used to construct a standard curve based on the absorbance of each solution. Then the average absorbance of each Rotenone concentration was substituted in the calculated trend line equation of the known BSA standard curve in order to estimate the protein concentration within each cell sample and to calculate the volumes of each sample needed to provide an estimated 15ug/ul of protein. Table 1 and 2, with their respective graphs, showed the linear equation used to determinate estimated protein concentration and the data calculated for each sample chosen to test for SDS-PAGE and Western Blot analysis.

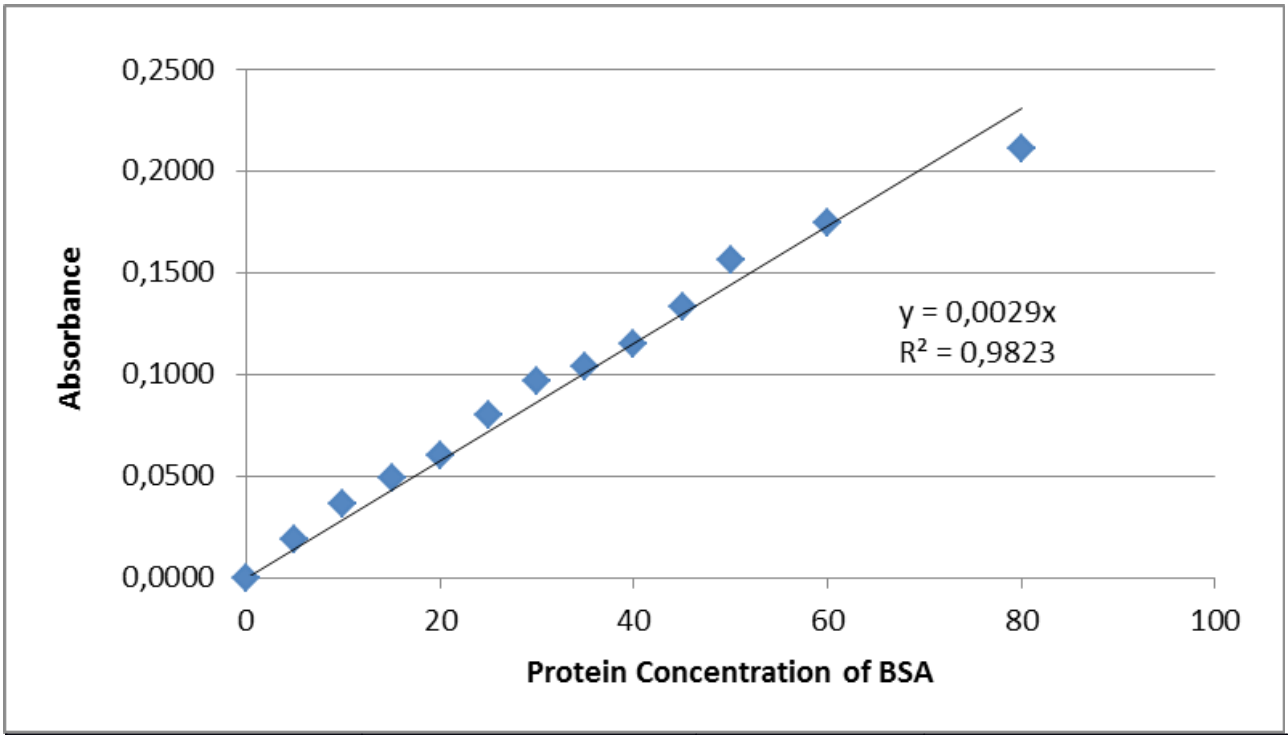

SH-SY5Y sample 1			
Rotenone Concentration	**Average Abs at 750 nm**	**Protein (ug/ul)**	**Volume (15ug protein)**
0 uM	0,1090	1,103	14
0,1 uM	0,1190	1,448	10
0,5 uM	0,0913	0,494	30
2,5 uM	0,1090	1,103	14

Table 1 : BSA standard curve and table of values as a result of the protein estimation from the first sample of Rotenone-treated SH-SY5Y cells. The last column represent the calculated volumes needed to provide an estimated 15ug/ul of protein.

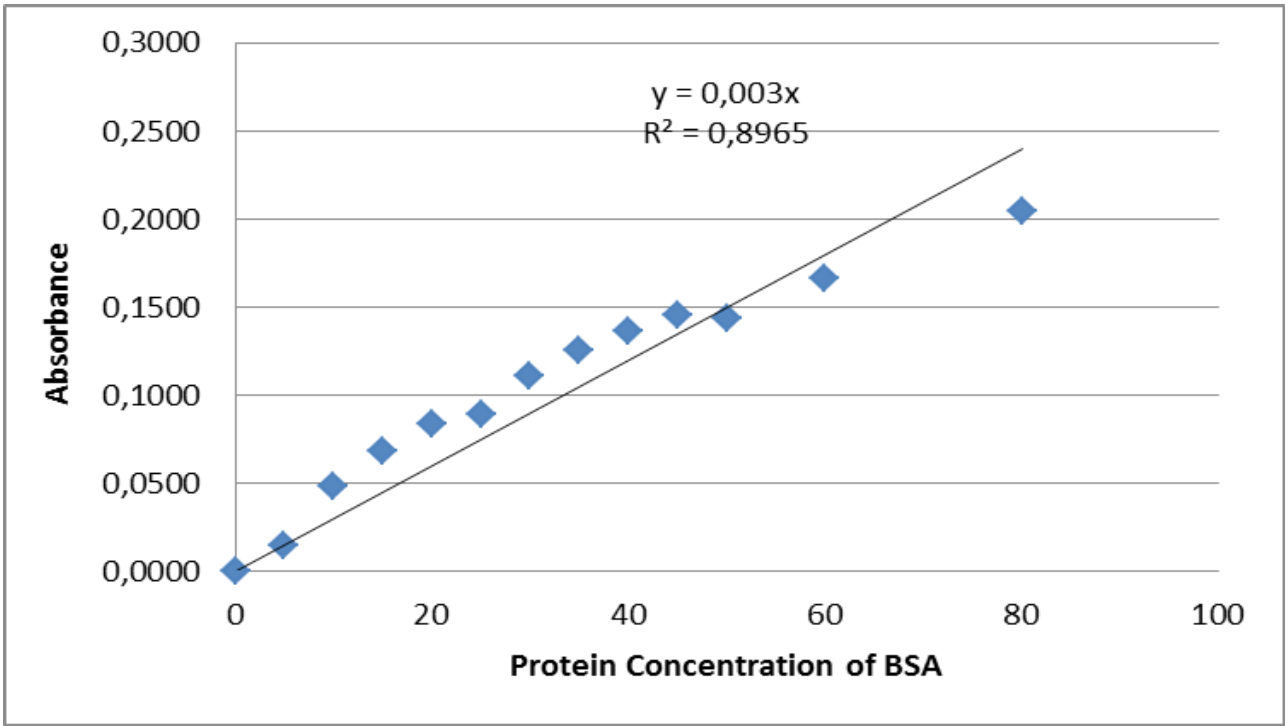

SH-SY5Y sample 2			
Rotenone Concentration	**Average Abs at 750 nm**	**Protein (ug/ul)**	**Volume ul (15ug protein)**
0 uM	0,10200	0,956	16
0,1 uM	0,10200	0,956	16
0,5 uM	0,09533	0,733	20
2,5 uM	0,08933	0,533	28

Table 2 : BSA standard curve and table of values as a result of the protein estimation from the second sample of Rotenone-treated SH-SY5Y cells. The last column represent the calculated volumes needed to provide an estimated 15ug/ul of protein.

Estimated proteins were then ran by SDS-PAGE in order to separate all the proteins within the cell samples by size. A protein standard ladder was loaded alongside our samples allowing to determinate which band represented the size of the target proteins.

Once the proteins run was finished, the gel was transferred onto a nitrocellulose membrane by a Semi-Dry Western Blotting, ideal for detecting proteins with a lower molecular weight that bound to the membrane by hydrophobic interactions. The protein bands of each lane on the membrane were initially visualized by a reversible Copper Stain (Figure 10). In order to cut the nitrocellulose in two sections for the Western Blot analysis, the standard ladder was used to determinate which was the appropriated band, visible by Copper Stain, of each target protein: based on the published literature, DJ-1 has been found to be around 20kDa and Nrf2 to be around 68kDa. Both sections of the membrane were first incubated with their respective primary antibodies that would bind specifically to DJ-1 and Nrf2, then with a secondary Blocking solution containing anti-IgG rabbit antibodies that allowed to visualize the target protein bands on the nitrocellulose by alkaline phosphate detection (Figure 11 and Figure 12).

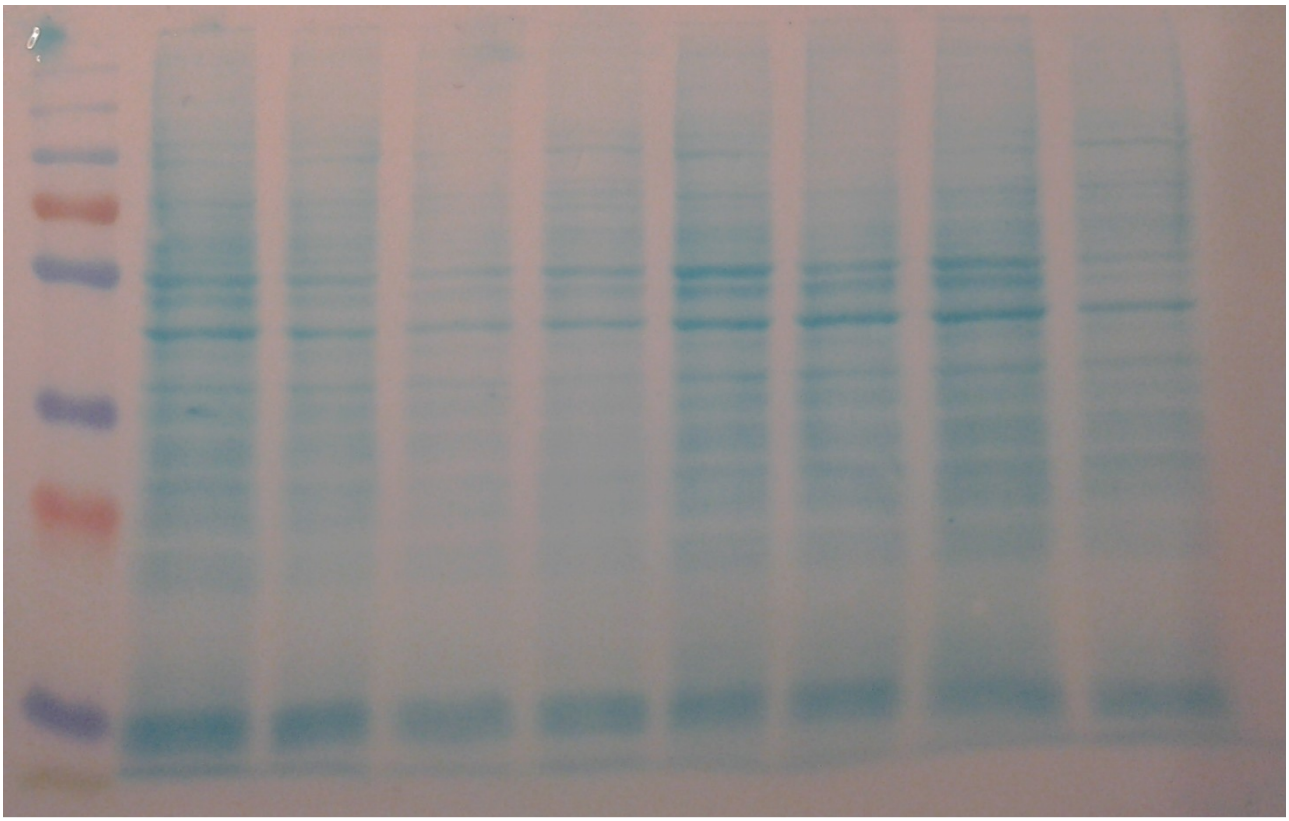

Figure 10 : Image of reversible Copper Stain performed after nitrocellulose membrane transfer in order to check if transfer was successful and to appropriately cut the membrane for the following Western Blotting. Lines 1-4 consist of the first SH-SY5Y cells sample, lines 5-8 consist of the second sample. The start of each line is the control (lanes 1 and 5) then it works up to 0.1uM, 0.5uM, and 2.5uM of Rotenone.

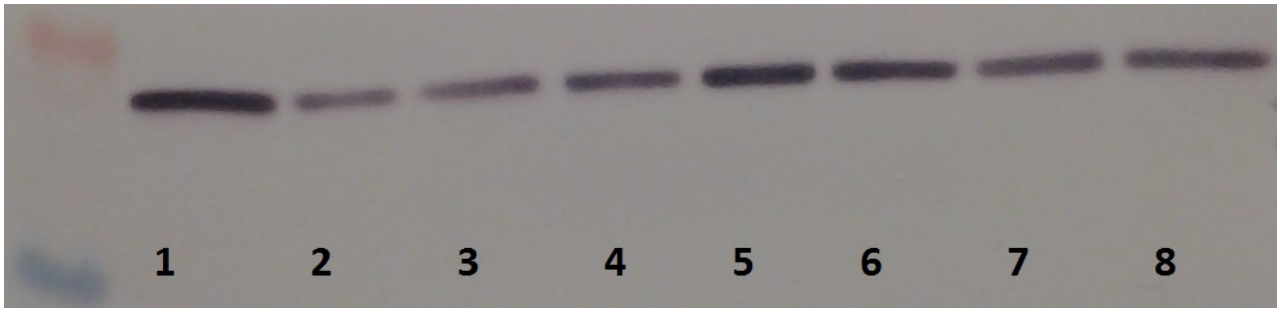

Figure 11 : Blot of mitochondrial protein DJ-1 (20kDa) in Rotenone treated SH-SY5Y cell samples. Lines 1-4 consist of the first SH-SY5Y cells sample, lines 5-8 consist of the second sample. The start of each line is the control (lanes 1 and 5) then it works up to 0.1uM, 0.5uM, and 2.5uM of Rotenone. Lines 1 and 5 representing the control have very intense bands.

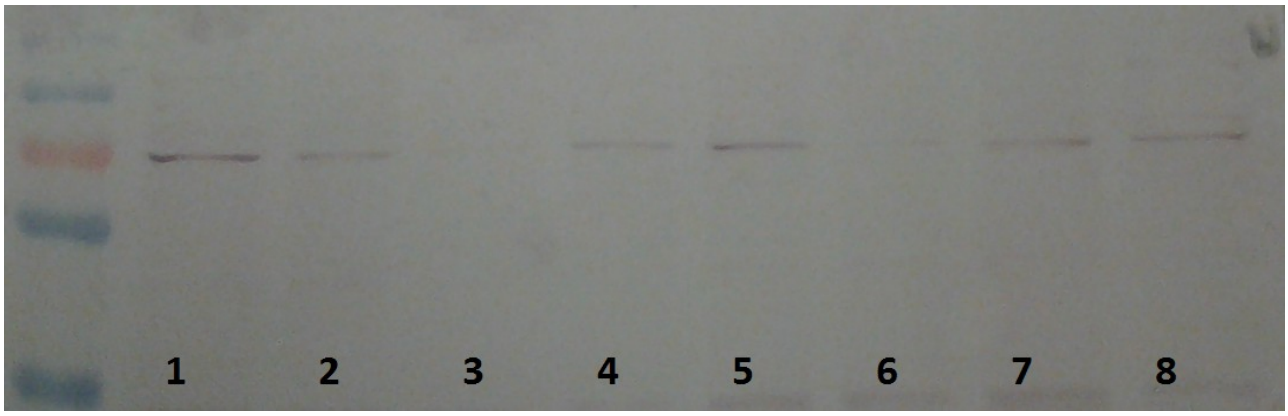

Figure 12 : Blot of mitochondrial protein Nrf2 (68kDa) in Rotenone treated SH-SY5Y cell samples. Lines 1-4 consist of the first SH-SY5Y cells sample, lines 5-8 consist of the second sample. The start of each line is the control (lanes 1 and 5) then it work up to 0.1uM, 0.5uM, and 2.5uM of Rotenone.

Visually, the membrane showing DJ-1 has very intense bands at Rotenone 0uM concentration (lane 1 and lane 5) but only in the second sample (lanes 5-8) a decrease of the boldness of the bands can be seen as a rise of the Rotenone concentration. The membrane exhibiting Nrf2 did not show much variability between bands, probably because of the low intensity of the dye, except for the Rotenone 0uM samples (lane 1 and lane 5) where bands are slightly more intense. Therefore lane 3 (Rotenone 0.5uM sample) and lane 6 (Rotenone 0.1uM sample) showed tiny bands that were almost invisible.

Suddenly, volumes of each protein were measured in an imaging system based on the band size and band colour intensity (BioRad ChemiDOC). DJ-1 volumes did not show variability between treatments, except for 2.5uM that in both samples were higher than the control (Figure 13). Therefore neither Nrf2 volumes showed a particular variability linked to Rotenone concentrations: in both samples they dropped at 0.1uM and 0.5uM Rotenone, then they increase at 2.5uM Rotenone but with two different patterns (Figure 14).

In order to determine a possible link between the two target proteins, a ratio of DJ-1 to Nrf2 was calculated using each measured integrated volume and summarised in Table 3. We expected to found a proportional correspondence between proteins volumes, as DJ-1 is a watch of Rotenone-induced oxidative stress that activates Nrf2 letting its translocation in the nucleus, but actually our results were not linked.

Unfortunately this experiment was not successful, thus any conclusions could not be supported by unclear results. Probably the lack of a Loading Control did not allow us to check that the lanes have been evenly loaded with sample or to quantify the protein amounts in each lane if even the transfer have not occurred.

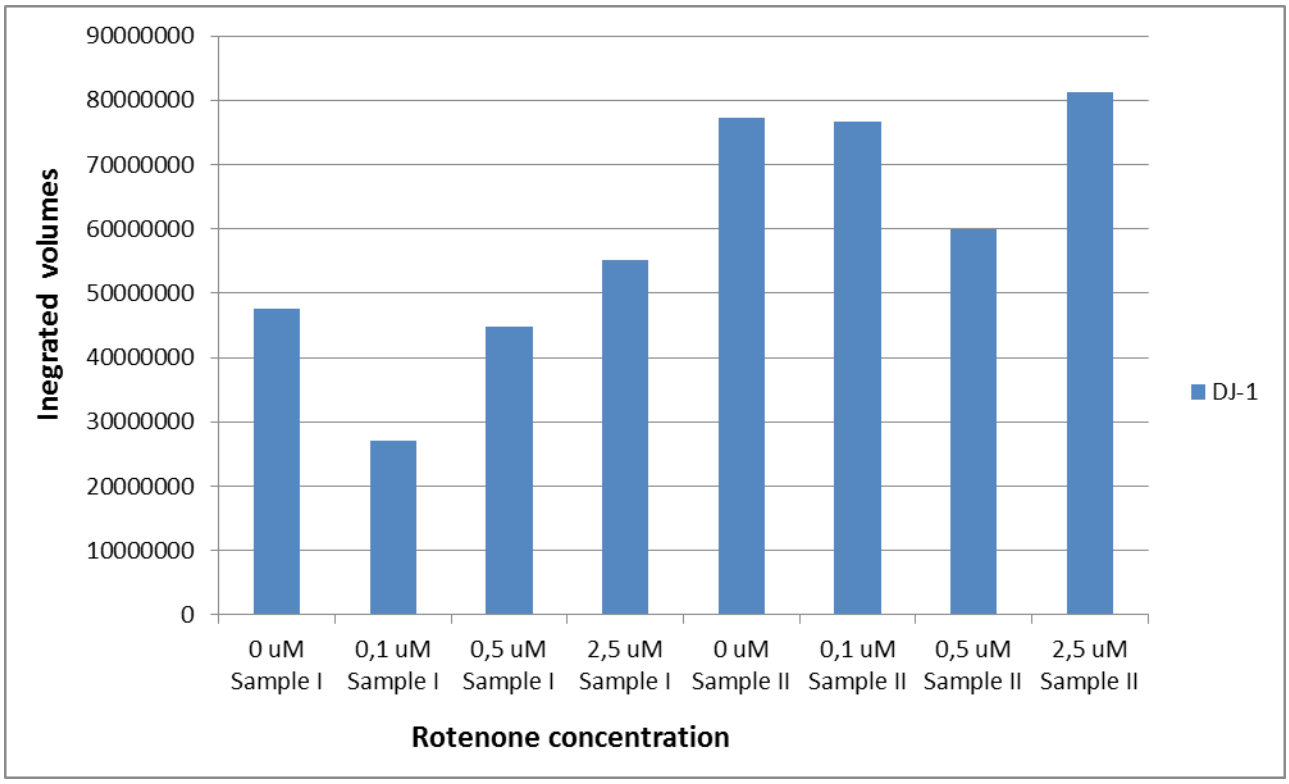

Figure 13 : Graphical representation of DJ-1 integrated volumes measured from blots by imaging system.

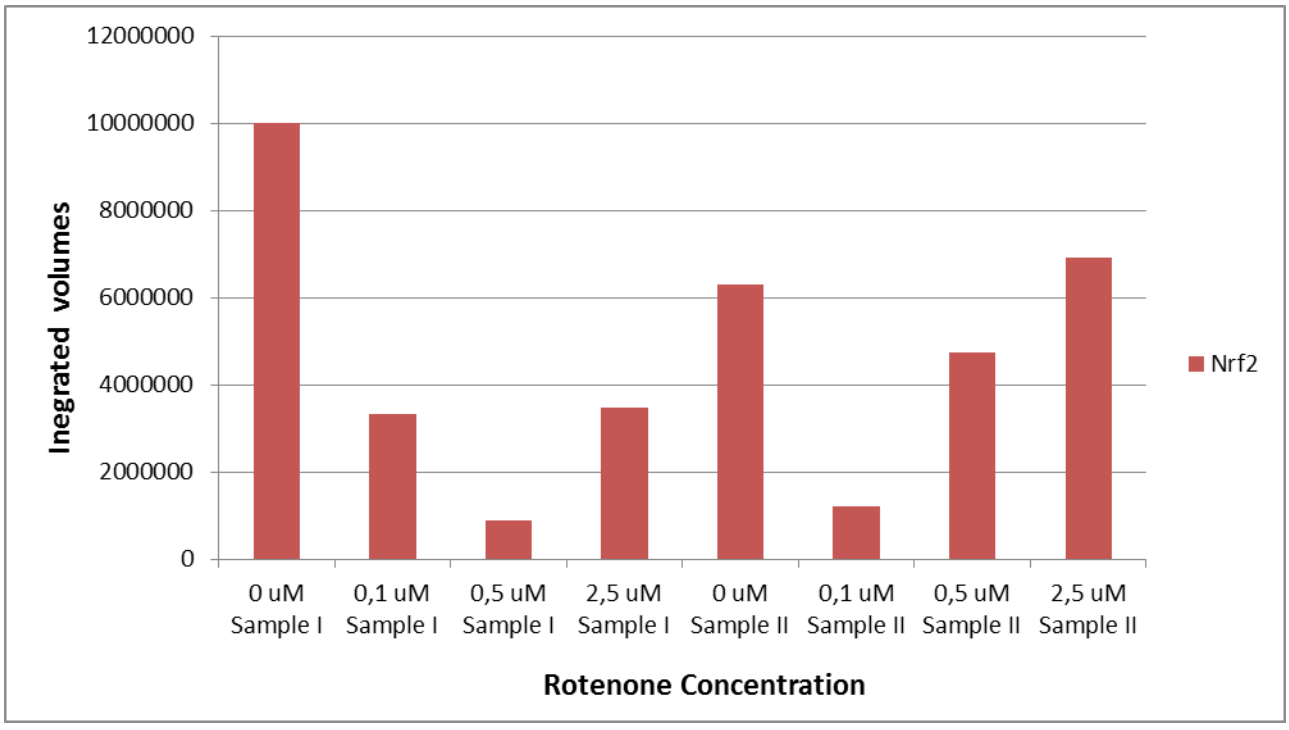

Figure 14 : Graphical representation of Nrf2 integrated volumes measured from blots by imaging system.

Sample I				
Rotenone Treatment	**DJ-1 Volume Integr.**	**Nrf2 Volume Integr.**	**Ratio**	**Normalised**
0 uM	47670980	10016805	4,7591003	1
0,1 uM	27101736	3334449	8,1278004	1,70784389
0,5 uM	44835703	892600	50,230454	10,5546112
2,5 uM	55160469	3472800	15,883572	3,33751569
Sample II				
Rotenone Treatment	**DJ-1 Volume Integr.**	**Nrf2 Volume Integr.**	**Ratio**	**Normalised**
0 uM	77302043	6299200	12,271724	1
0,1 uM	76649628	1210900	63,299718	5,15817649
0,5 uM	59974848	4731951	12,674444	1,03281692
2,5 uM	81266172	6926640	11,732409	0,95605221

Table 3: Summary of measured integrated volumes and ratio of DJ-1 and Nrf2 present in SH-SY5Y Western blot analysis.

3.3 U-87 MG cultured medium protection of SH-SY5Y cells against Rotenone-induced cell death.

In order to investigate how Glial cells attend particular neuronal dysfunctions like mitochondrial damage, the human glioblastoma astrocytoma U-87 MG cell line was incubated in EMEM medium for 72 hours and the produced medium was collected, centrifuged and stored at 4°C before being used to treat SH-SY5Y cells. Neuroblastoma cells were first placed on a 96-wells plate and allowed to grow for 3 days with single DMEM medium. Then half plate medium was aspirated and replaced with a mixture of DMEM and EMEM medium (1:1) treated with 0, 0.1, 0.5, 2.5 and 10uM of rotenone. The medium of the other half-side of the plate was aspirated and replace a mixture of DMEM and GLIOMA cultured medium (1:1) treated with the same five rotenone concentrations. After 48 hours the cell viability was measured by the MTT reduction.

As shown in Figure 16, with EMEM medium the percent cell viability of SH-SY5Y cells decreased from 100% at the control to 7% at 10uM rotenone concentration, conversely with GLIOMA cultured medium the cell viability decreased from 100% to 22%. Therefore both 2.5uM and 10uM treatments exhibited higher cell survival with GLIOMA cultured medium (23 and 22%) comparing with EMEM medium (15 and 7%). These percentages were confirmed by the images in Figure 15, where it was possible to see a few healthy cells at the higher concentrations of rotenone (Figures 15-H and 15-L).

Data collected were considered statistically significant by the use of a Student T-test. All concentrations of rotenone of both media treatments contained a p-value < 0.05, except for 0.1uM rotenone which did not have a statistically significant drop in percent cell viability compared to the control.

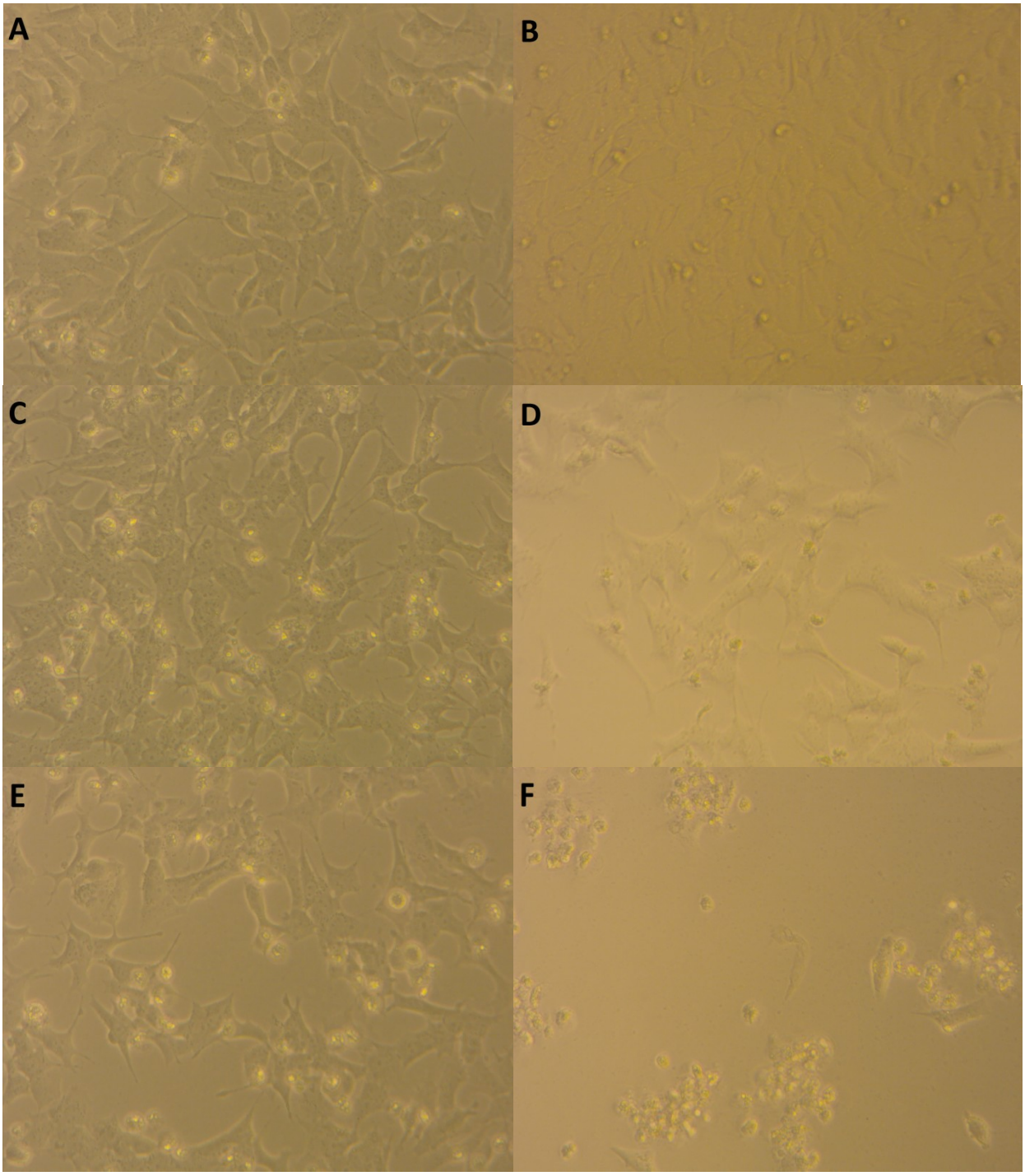
A
B
C
D
E
F

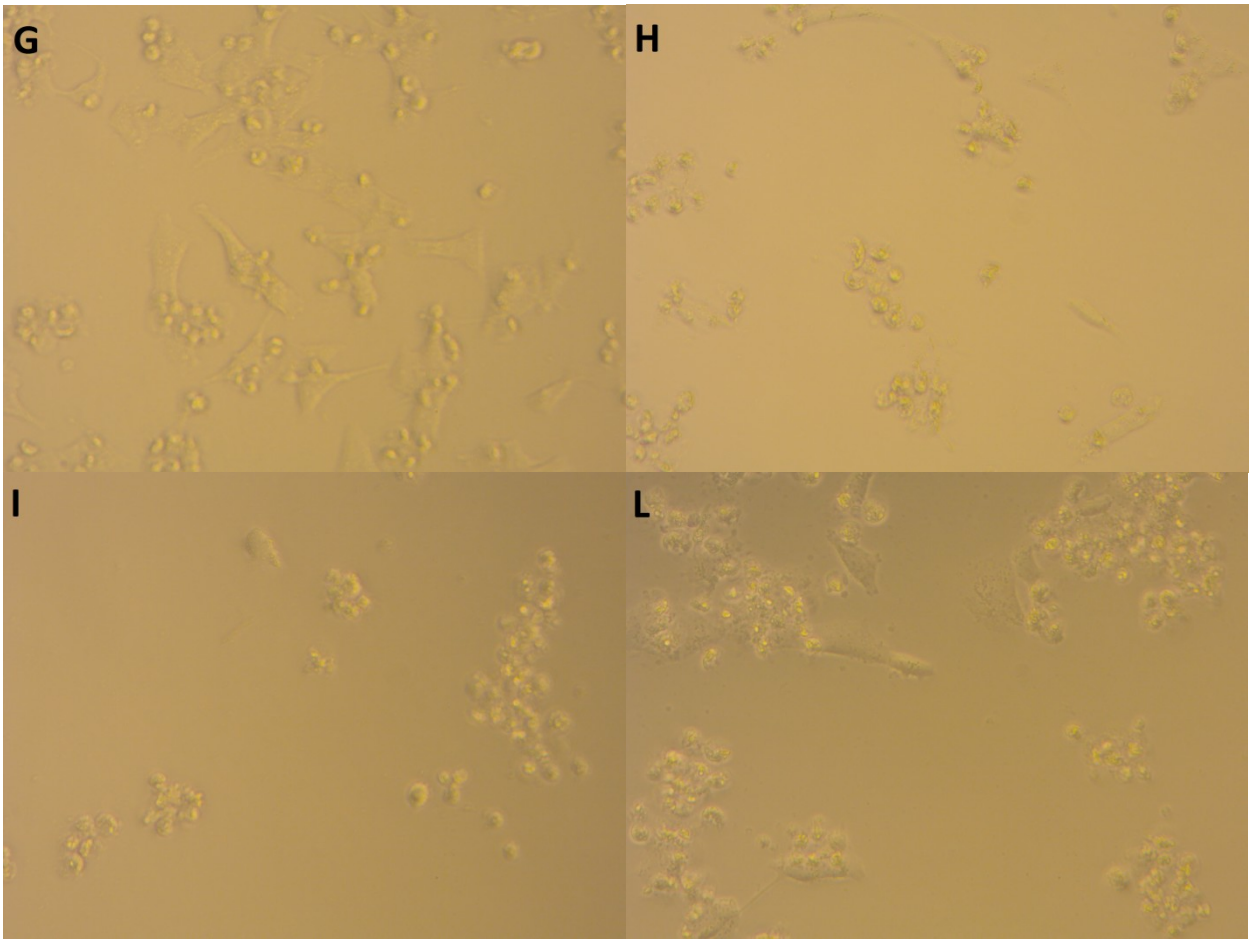

Figure 15 : Pictures of human neuroblastoma SH-SY5Y cells after co-treatment with Rotenone and cultured medium from human glioma U-87 MG cell line.
A) cells co-treated with Emem medium and 0uM of Rotenone, used as a first control; B) cells co-treated with Glioma medium and 0uM of Rotenone, used as a second control C) cells co-treated with Emem medium and 0.1uM of Rotenone; D) cells co-treated with Glioma medium and 0.1uM of Rotenone; E) cells co-treated with Emem medium and 0.5uM of Rotenone; F) cells co-treated with Glioma medium and 0.5uM of Rotenone; G) cells co-treated with Emem medium and 2.5uM of Rotenone; H) cells co-treated with Glioma medium and 2.5uM of Rotenone; I) cells co-treated with Emem medium and 10uM of Rotenone; L) cells co-treated with Glioma medium and 10uM of Rotenone.

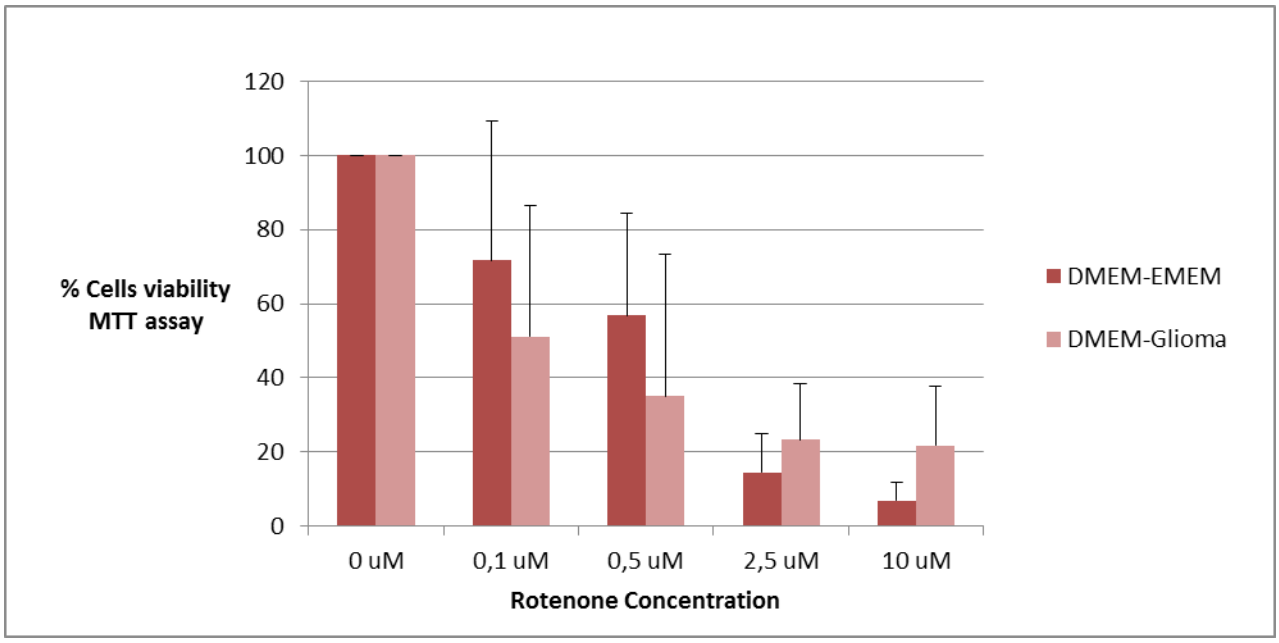

Figure 16 : Graphical representation of MTT assay performed on human neuroblastoma SH-SY5Y cells after 48 hours co-treatment with Rotenone and cultured medium from human glioma U-87 MG cell line.

3.4 U-87 MG cultured medium modulation of SH-SY5Y cells proliferation.

Since the significant results obtained with the Rotenone treatment, the last purpose was to investigate if SHSY5Y cells modified their proliferation pattern in presence of Glioma media.

The first approach was to plate Neuroblastoma cells in a 96-well plate with three different kinds of medium: DMEM medium as a control, a mixture of DMEM and EMEM medium (1:1), a mixture of DMEM and Glioblastoma cultured medium (1:1). MTT viability assay was performed after 1 day, 2 days and 3 days of growth.

Looking at the pictures (Figures 17, 18 and 19) it has been possible to find a visual higher concentration of cells with DMEM-EMEM medium treatment and DMEM-Glioma medium treatment compared to the control of each day of the experiment.

As shown in the graphical representation in Figure 20, the percent cell viability of SHSY5Y cells increased from the control in both DMEM-EMEM medium and DMEM-Glioma medium treatments and mostly after 1 day: the 100% cell viability of the control rose to 331% with EMEM medium and to 240% with Glioma medium. After 2 and 3 days, the cell viability of the cells in EMEM and Glioma was decreased from the first treatment but still higher than the control. Therefore in each case the percent viability of the cells grown with Glioma medium was lower than the percent viability of the ones grown with EMEM medium, with a drop of 91% after 1 day, 89% after 2 days and 78% after 3 days.

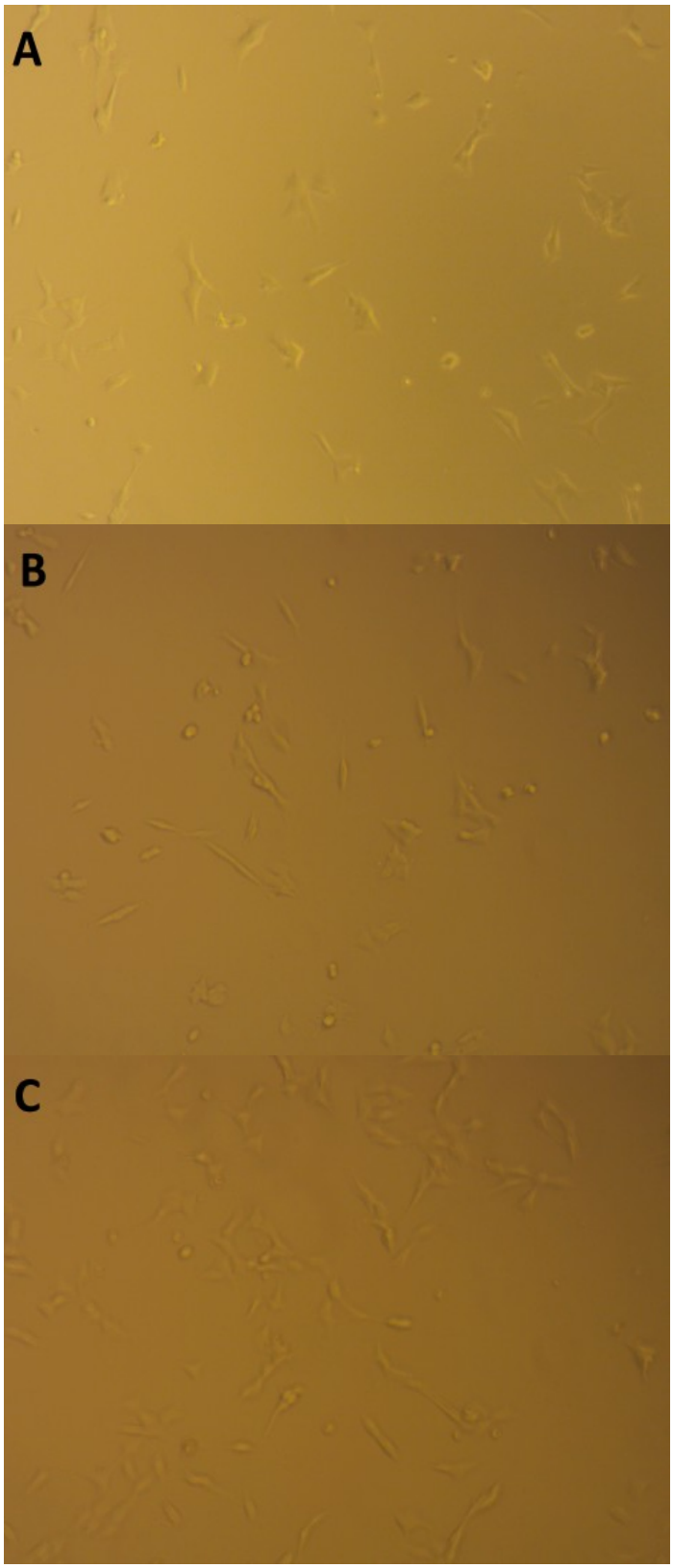

Figure 17 : Pictures of human neuroblastoma SH-SY5Y cells after 1 day of growth in plates with different kinds of media: A) only DMEM medium as the control, B) DMEM medium and EMEM medium, C) DMEM medium and cultured medium from Human Glioma U-87 MG cell line.

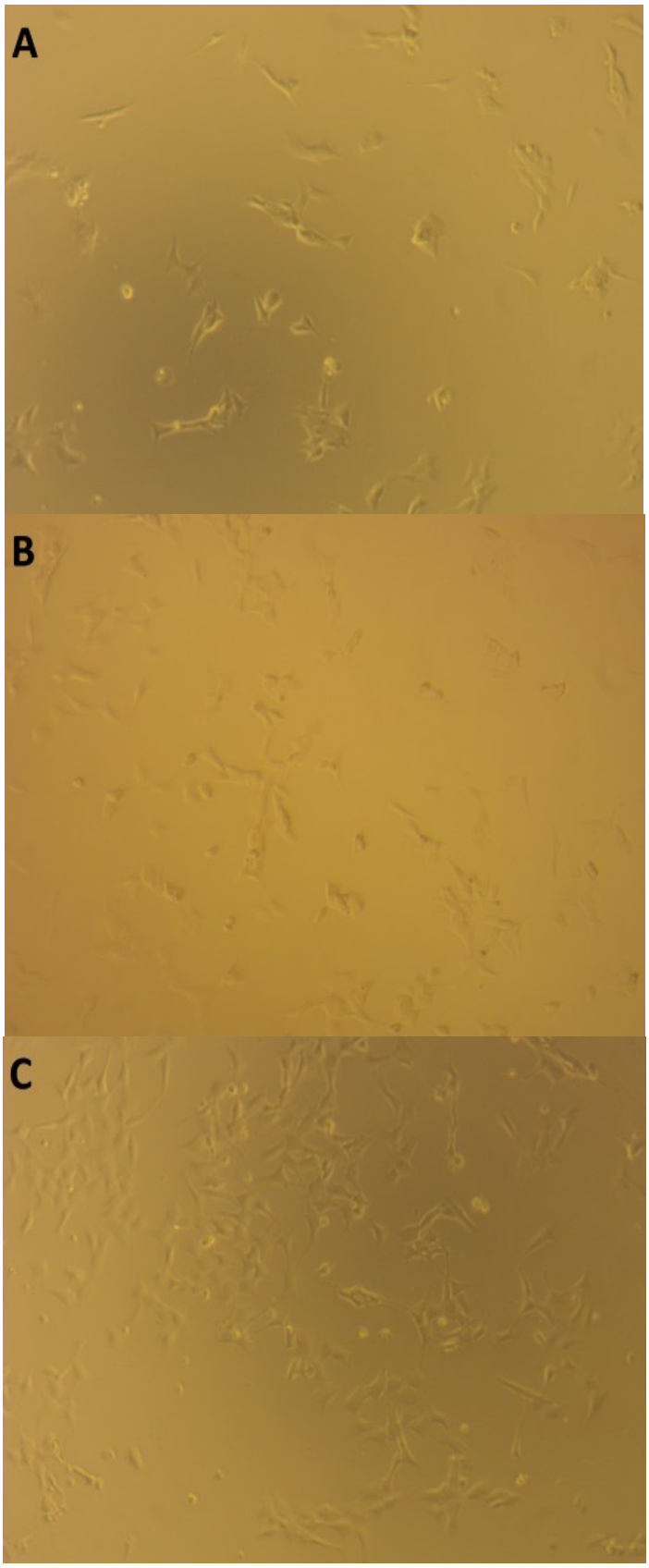

Figure 18 : Pictures of human neuroblastoma SH-SY5Y cells after 2 days of growth in plates with different kinds of media: A) only DMEM medium as the control, B) DMEM medium and EMEM medium, C) DMEM medium and cultured medium from Human Glioma U-87 MG cell line.

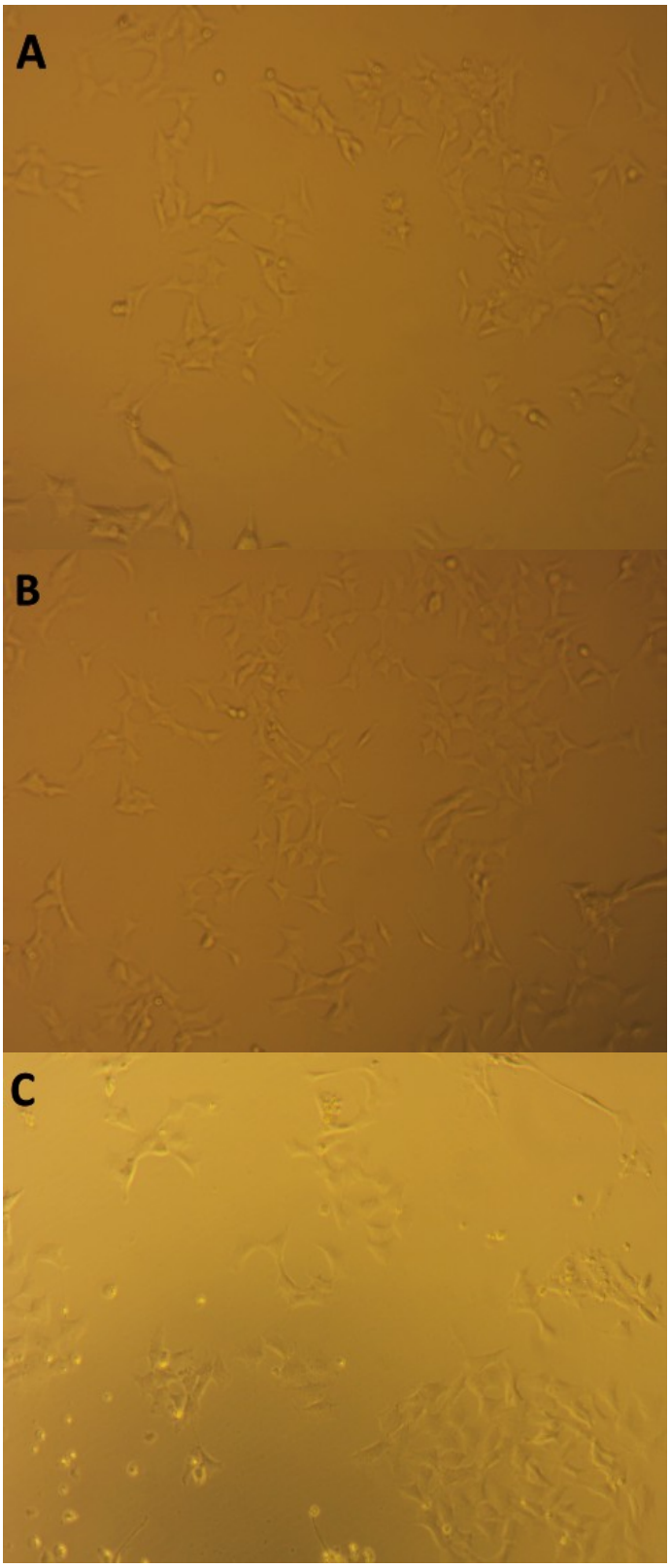

Figure 19 : Pictures of human neuroblastoma SH-SY5Y cells after 3 days of growth in plates with different kinds of media: A) only DMEM medium as the control, B) DMEM medium and EMEM medium, C) DMEM medium and cultured medium from Human Glioma U-87 MG cell line.

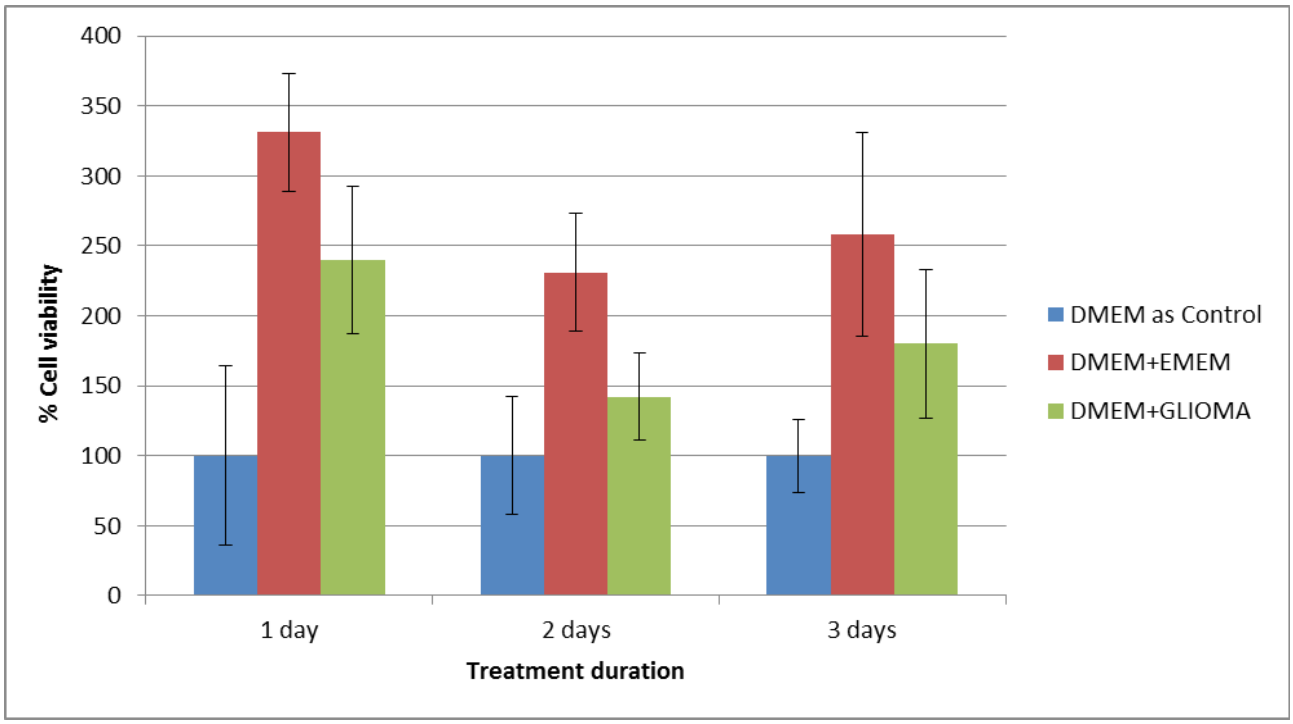

Figure 20 : Graphical representation of MTT assay performed on human neuroblastoma SH-SY5Y cell line grown for 1-2-3 days in plates with different types of medium: DMEM medium as a control, DMEM medium mixed with EMEM medium and DMEM medium mixed with cultured medium from human glioma U-87 MG cell line.

The second approach pertained the incubation of SH-SY5Y cells in T-25 flasks with the three types of medium of the previous experiment: DMEM as a control, DMEM and EMEM, DMEM and glioblastoma cultured medium. MTT viability assay was performed after 2 and 3 days of growth as a parameter of mitochondrial metabolic activity, while a cell count was previously performed to estimate the cell number of each flask. Cells were detached from the flask by a cell scraper, a few microliters of the resulting suspension were diluted and used for the cell count then the rest of the suspension was incubated with MTT.

As exhibited in Figures 21 and 22, there was not a relevant difference in the cell density between the treatment after two days as after three. However, cells grown for three days with the GLIOMA medium (Figures 21-C) presented more death cells and more signs of apoptosis compared to the cells of the control and the cells within EMEM. This would be explained by the lack of nourishment that characterized the medium already cultured over three days within glioblastoma cells.

The visual cell density was then compared with a cell count. As shown in Figure 23, after two days of treatment the cells grown with GLIOMA medium were 2250/ul whereas control cells were 2130/ul and cells grown with EMEM medium were 1780/ul. As expected from the visual analysis, after three days the concentration of the cells grown with GLIOMA medium was found very reduced (1490/ul) and also control cells were less than the day before (1630/ul). Interestingly cells grown with EMEM medium were found to be slightly increased from 1780/ul to 1940/ul.

Figure 24 is a graphical representation of the percent cell viability obtained by MTT assay in order to compare cell concentration with cell metabolic activity. It did not show much variability between treatments except for the GLIOMA medium, where the cell viability after two days was 11% lower than the control and 15% than EMEM medium.

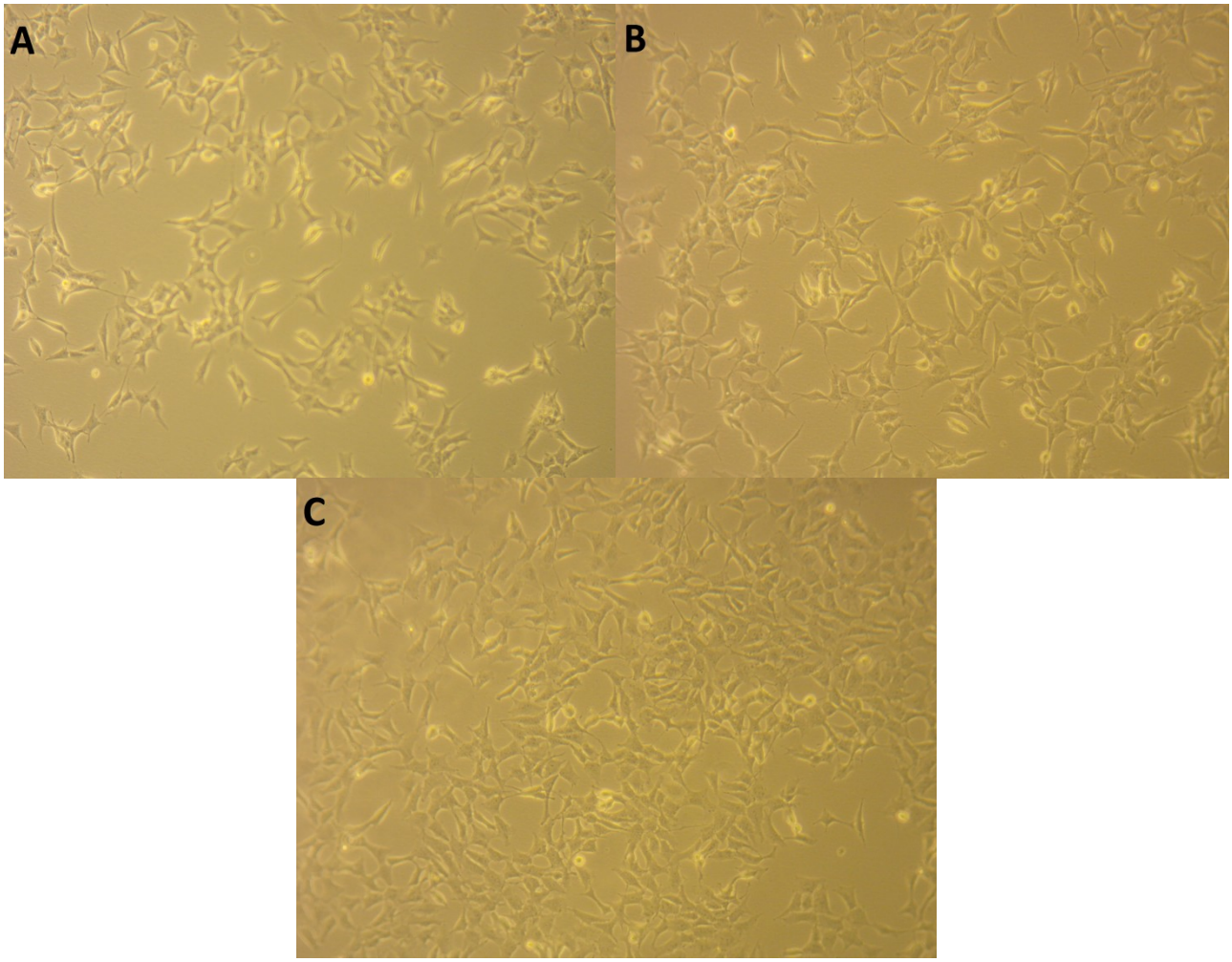

Figure 21 : Pictures of human neuroblastoma SH-SY5Y cells after 2 days of growth in different kind of media: A) only DMEM medium, B) DMEM medium and EMEM medium, C) DMEM medium and cultured medium from human glioma U-87 MG cell line.

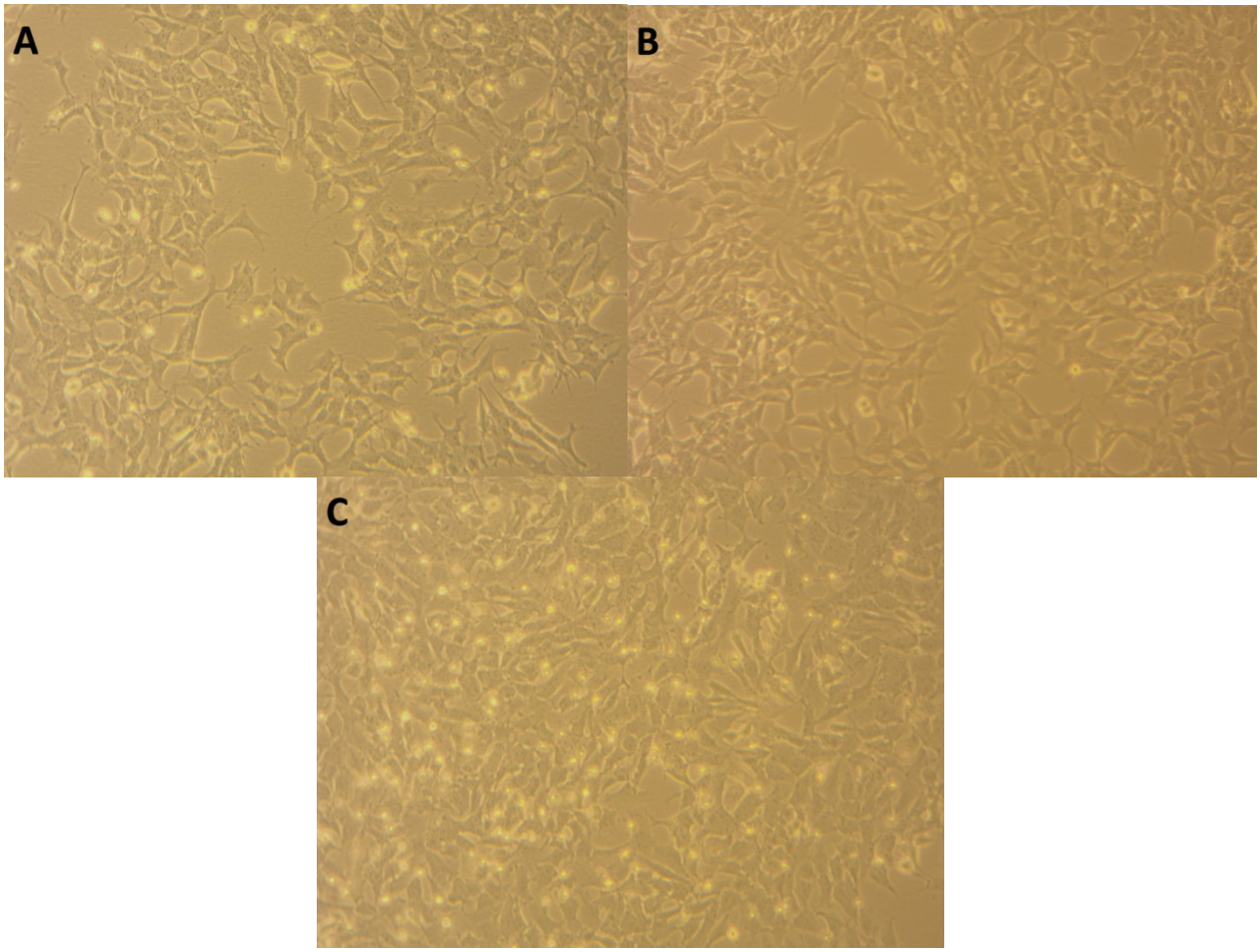

Figure 22 : Pictures of human neuroblastoma SH-SY5Y cells after 3 days of growth in different kind of media: A) only DMEM medium, B) DMEM medium and EMEM medium, C) DMEM medium and cultured medium from human glioma U-87 MG cell line.

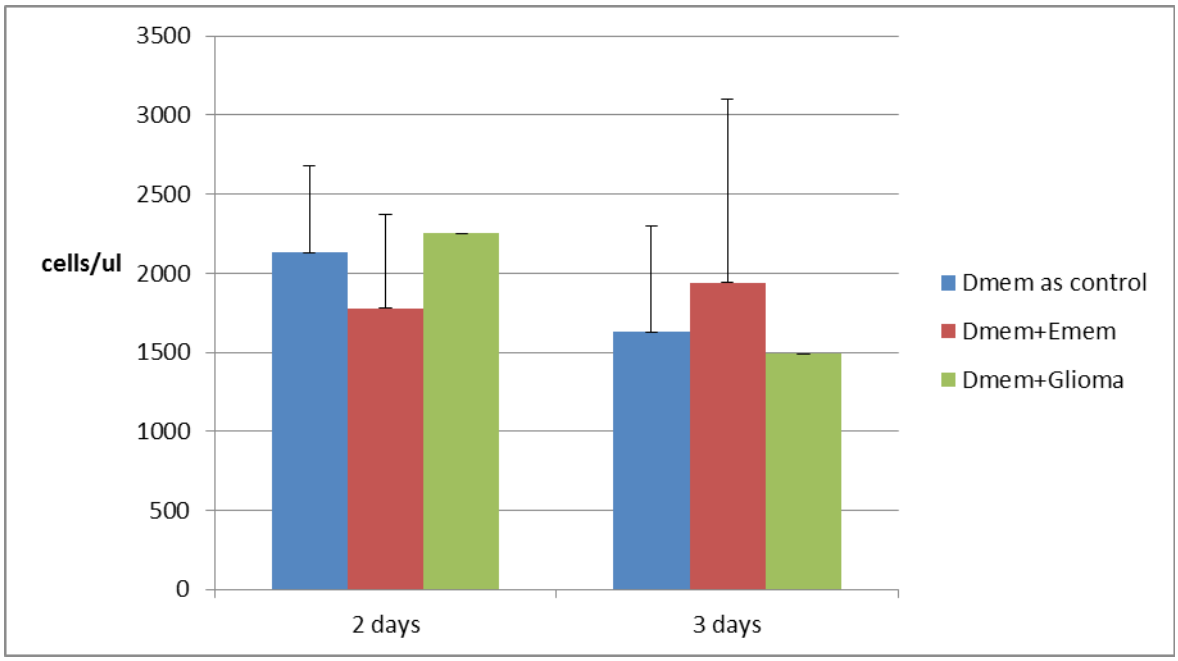

Figure 23 : Graphical representation of the cell count performed on human neuroblastoma SH-SY5Y cell line grown in three different kind of flasks: with DMEM medium as a control, with EMEM medium and with cultured medium from human glioma U-87 MG cell line.

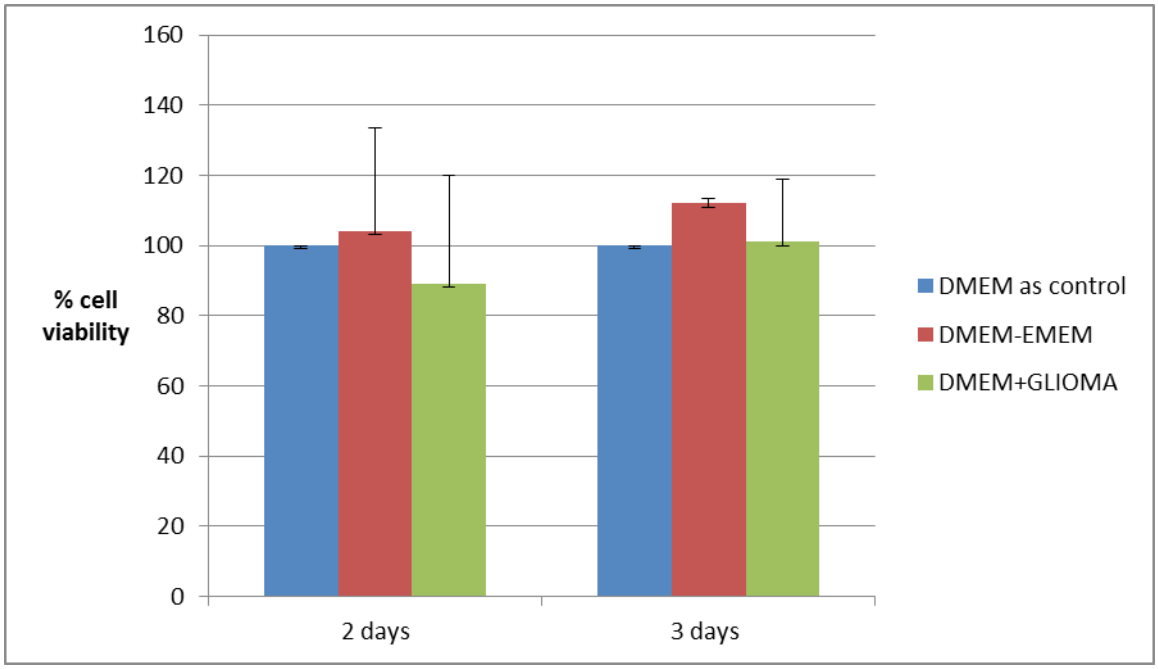

Figure 24 : Graphical representation of MTT viability assay performed on human neuroblastoma SH-SY5Y cell line grown in three different kind of flasks: with DMEM medium as a control, with EMEM medium and with cultured medium from human glioblastoma U-87 MG cell line.

4. CONCLUSIONS

The mitochondrial protein DJ-1, the transcription factor protein Nrf2 and the neural support glial cells are particularly popular in recent studies involving the possibility that they could potentially play a role in altering the neurodegenerative effects of PD.

In this project, we set out to investigate how DJ-1 and Nrf2 are affected by the known parkinsonian reagent rotenone in a neuronal cell model of human neuroblastoma SH-SY5Y cells. We also evaluated whether or not the presence of a medium collected from a Human glioblastoma astrocytoma U-87 MG culture could spur proliferation or provide protection against rotenone-induced apoptosis in SH-SY5Y cells.

Primarily, we tested how exactly the SH-SY5Y cells were affected by rotenone. We then compared the rotenone effects against the effects of the known oxidant H2O2 using MTT and Neutral Red viability assays. Previous studies (Cassarino et al., 1997. Betarbeth et al., 2000. Kurshnareva et al., 2002) determined that rotenone toxicity in Neuroblastoma cells depends on a direct interaction with Complex I, which partially inhibits the enzyme and leaks electrons enhancing ROS production. Therefore cells expressing the rotenone-insensitive single-subunit NADH dehydrogenase of yeast (NDI1), that acts as a copy for the entire mammalian Complex I, were resistant to rotenone toxicity (Sherer at al. 2003). Thus rotenone toxicity indeed appears to result primarily from oxidative damage.

In both cases the cell viability decreased as expected as the concentrations of rotenone and H2O2 became higher. The two higher concentrations of rotenone (2.5uM and 10uM) and three higher concentration of H2O2 (500uM, 1000uM and 2000uM) were also immediately affected physically. Looking at the images they were able to induce cellular apoptosis, with a considerable change in overall cellular morphology and with little remaining viable cells. So we were able to conclude that the higher rotenone and H2O2 concentrations which were found to not be statistically significant, were simply due to the fact that overall cell death had occurred in those case and both viability assays were unable to correctly distinguish cell death levels.

It is important to note that there was an observed colour change in the media of the cells in the 96-well plate. As opposed to the normal orange coloration of the media due to the presence of phenol red, the media in the 0.1uM and 0.5uM rotenone-treated cells had turned yellow. It is possible that due to the mitochondrial complex 1 inhibition from the rotenone thus the cells were using the glucose and other nutrients present in the media to undergo glycolysis in order to maintain energy production within the cells.

We next investigated if the presence of Rotenone on SH-SY5Y cells had an effect on DJ-1 and Nrf2, and if there was a link between DJ-1 and the activation of Nrf2 for the Nrf2-ARE pathway. In a study performed by Clements et al. in 2006, they demonstrated that DJ-1 helps to stabilize Nrf2 and triggers the activation of the Nrf2-ARE pathway: in fact DJ-1 prevents Keap1 from binding to Nrf2 and allows its translocation into the nucleus from the cytoplasm. Likewise, an observed decrease in DJ-1 also exhibited a decrease in other anti-oxidative proteins regulated by the Nrf2-ARE pathway, which led the researchers to believe that DJ-1 played a role in the overall activation of this combative response.

We expected to find a correspondence between DJ-1 and Nrf2 band intensities, calculated from the Western Blot, activated by the rotenone-induced oxidative stress. Unfortunately our results did not show a proper pattern that could confirm the rise of the measured band intensities as the Rotenone concentration became higher, thus we could not demonstrate experimentally our assumptions.

Assuming that Glial cells support synaptic contacts and maintain the signaling abilities of neurons, previous studies have analysed how these cells are activated as a result of neuronal conditions of stress: modulating synaptic action by controlling the uptake of neurotransmitters, modulating the rate of nerve signal propagation, providing a scaffold for some aspects of neural development, and maintain, in a variety of ways, an appropriate chemical environment for neuronal signaling ("Studying the Nervous Systems of Humans and Other Animals" Purves et al., 2004). In order to investigate how Glial cells attend particular neuronal dysfunctions like mitochondrial damage, a human glioblastoma U-87 MG cell line was cultivated in order to produce a medium rich of growth factors and signal molecules thought to be useful for neural survival. MTT viability assays were performed again with the presence of Glioma cultured medium compared to the un-cultured EMEM medium and they appeared to play a role in combating cellular apoptosis. In fact, at the highest concentrations of Rotenone used, 2.5uM and 100uM respectively, Glioma medium had the most success in fighting off apoptosis, whereas at the middle concentration was not as successful as the EMEM control medium. This leads us to believe that the cells treated with those two concentrations of Rotenone (0.1uM and 0.5uM) were effectively not enough injured to trigger an intensive defensive response.

Our results are consistent to a study performed by Duckhande et al. in 2013, where they demonstrated the neuroprotective role of glioblastoma U-87 secreted factor against neuroblastoma SK-N-SH glutathione depletion-induced apoptosis. They indeed considered astrocytes factors as potential candidates for rescuing neurons undergoing oxidative stress.

Finally, for our last set of experiments we set out to investigate if glial cells attended also in neural proliferation. Consequently we incubated neuroblastoma cells with DMEM medium as a control, a mixture of DMEM and EMEM, a mixture of DMEM and glioblastoma cultured medium in 96-well plates for 1,2,3 days and in T-25 flasks for 2 and 3 days.

Observing our results, it would seem that the Glioma medium used did not appear to provide much difference in spurring the cell growth. In fact both MTT viability assay and cell count performed on the cells grown in the flasks showed an increased viability in both EMEM and Glioma treatments compared to the control. Moreover MTT assay performed on the plates did not show variability or particular differences between the cells grown in the three mixture medium during all the three treatment periods.

We could then confirm the results of the previous experiment: glioblastoma medium did not containe molecules that promote proliferation but that support and defend neural cells against oxidative injuries indeed.

It is interesting to notice that SH-SY5Y cells viability, most of the times, was higher when they were cultured with EMEM medium than with either the control or the Glioma medium. This can be explained by the fact that neuroblastoma cells found in EMEM a better culture medium and that the cultured Glioma medium was less rich of nourishments, as it was already cultured for 3 days within U-87 MG cells, so the cells had to grow in extreme conditions.

Given the chance to continue with this experiment, it would be interesting to see if the results for our MTT viability assays would change with the introduction of U-87 MG cultured-medium pre-treatment in the cultures. Therefore it would be beneficial to repeat the analysis of DJ-1 and Nrf2 levels within SH-SY5Y cells and to test if they would change with samples co-treated with glioblastoma cultured-medium and Rotenone. Finally, in order to see which results would be obtained after rotenone treatments, it would be of interest to set similar experiments on U-87 MG cells and subsequently to analyse which neuroprotective molecules would be found within the glioblastoma cultured-medium.

Further studies that investigate glial cells factors as well other avenues that work toward activating the Nrf2-ARE pathway, could further provide promising strategies against oxidative stress and neurodegeneration in Parkinson’s disease.

REFERENCES

Ariga H, Takahashi-Niki K, Kato I, Maita H, Niki T, Iguchi-Ariga SM. Neuroprotective function of DJ-1 in Parkinson's disease. Oxid Med Cell Longev. 2013;2013:683920.

Barroso N, Campos Y, Huertas R, Esteban J, Molina JA, Alonso A, Gutierrez-Rivas E, Arenas J. Respiratory chain enzyme activities in lymphocytes from untreated patients with Parkinson disease. Clin Chem. 1993 Apr;39(4):667-9.

Betarbet R, Sherer TB, MacKenzie G, Garcia-Osuna M, Panov AV, Greenamyre JT. Chronic systemic pesticide exposure reproduces features of Parkinson's disease. Nat Neurosci. 2000 Dec; 3(12):1301-6.

Blesa J, Trigo-Damas I, Quiroga-Varela A, Jackson-Lewis VR. Oxidative stress and Parkinson's disease. Front Neuroanat. 2015 Jul 8;9:91.

Bonifati V, Rizzu P, Squitieri F, Krieger E, Vanacore N, van Swieten JC, Brice A, van Duijn CM, Oostra B, Meco G, Heutink P. DJ-1(PARK7), a novel gene for autosomal recessive, early onset parkinsonism. Neurol Sci. 2003 Oct;24(3):159-60.

Braak H, Rüb U, Jansen Steur EN, Del Tredici K, de Vos RA. Cognitive status correlates with neuropathologic stage in Parkinson disease. Neurology. 2005 Apr 26;64(8):1404-10.

Büeler H. Impaired mitochondrial dynamics and function in the pathogenesis of Parkinson's disease. Exp Neurol. 2009 Aug;218(2):235-46.

Burté F, De Girolamo LA, Hargreaves AJ, Billett EE. Alterations in the mitochondrial proteome of neuroblastoma cells in response to complex 1 inhibition. J Proteome Res. 2011 Apr 1;10(4):1974-86.

Canet-Avilés RM, Wilson MA, Miller DW, Ahmad R, McLendon C, Bandyopadhyay S, Baptista MJ, Ringe D, Petsko GA, Cookson MR. The Parkinson's disease protein DJ-1 is neuroprotective due to cysteine-sulfinic acid-driven mitochondrial localization. Proc Natl Acad Sci U S A. 2004 Jun 15;101(24):9103-8.

Cassarino DS, Fall CP, Swerdlow RH, Smith TS, Halvorsen EM, Miller SW, Parks JP, Parker WD Jr, Bennett JP Jr. Elevated reactive oxygen species and antioxidant enzyme activities in animal and cellular models of Parkinson's disease. Biochim Biophys Acta. 1997 Nov 28;1362(1):77-86.

Chinta SJ, Andersen JK. Redox imbalance in Parkinson's disease. Biochim Biophys Acta. 2008 Nov;1780(11):1362-7.

Clements CM, McNally RS, Conti BJ, Mak TW, Ting JP. DJ-1, a cancer- and Parkinson's disease-associated protein, stabilizes the antioxidant transcriptional master regulator Nrf2. Proc Natl Acad Sci U S A. 2006 Oct 10;103(41):15091-6. Epub 2006 Oct 2.

Darios F, Corti O, Lücking CB, Hampe C, Muriel MP, Abbas N, Gu WJ, Hirsch EC, Rooney T, Ruberg M, Brice A. Parkin prevents mitochondrial swelling and cytochrome c release in mitochondria-dependent cell death. Hum Mol Genet. 2003 Mar 1;12(5):517-26.

Dauer W, Przedborski S. Parkinson's disease: mechanisms and models. Neuron. 2003 Sep 11;39(6):889-909.

Dawson TM, Ko HS, Dawson VL. Genetic animal models of Parkinson's disease. Neuron. 2010 Jun 10;66(5):646-61.

Dias V, Junn E, Mouradian MM. The role of oxidative stress in Parkinson's disease. J Parkinsons Dis. 2013;3(4):461-91.

Dukhande VV, Kawikova I, Bothwell AL, Lai JC. Neuroprotection against neuroblastoma cell death induced by depletion of mitochondrial glutathione. Apoptosis. 2013 Jun;18(6):702-12. doi: 10.1007/s10495-013-0836-4.

Fitzgerald JC, Plun-Favreau H. Emerging pathways in genetic Parkinson's disease: autosomal-recessive genes in Parkinson's disease--a common pathway? FEBS J. 2008 Dec;275(23):5758-66.

Hardy J, Cai H, Cookson MR, Gwinn-Hardy K, Singleton A. Genetics of Parkinson's disease and parkinsonism. Ann Neurol. 2006 Oct;60(4):389-98.

Hattori N, Shimura H, Kubo S, Wang M, Shimizu N, Tanaka K, Mizuno Y. Importance of familial Parkinson's disease and parkinsonism to the understanding of nigral degeneration in sporadic Parkinson's disease. J Neural Transm Suppl. 2000;(60):101-16.

Hoekstra JG, Cook TJ, Stewart T, Mattison H, Dreisbach MT, Hoffer ZS, Zhang J. Astrocytic dynamin-like protein 1 regulates neuronal protection against excitotoxicity in Parkinson disease. Am J Pathol. 2015 Feb;185(2):536-49.

Hwang O. Role of oxidative stress in Parkinson's disease. Exp Neurobiol. 2013 Mar;22(1):11-7.

Im JY, Lee KW, Woo JM, Junn E, Mouradian MM. DJ-1 induces thioredoxin 1 expression through the Nrf2 pathway. Hum Mol Genet. 2012 Jul 1;21(13):3013-24.

Junn E, Jang WH, Zhao X, Jeong BS, Mouradian MM. Mitochondrial localization of DJ-1 leads to enhanced neuroprotection. J Neurosci Res. 2009 Jan;87(1):123-9.

Kim Y, Park J, Kim S, Song S, Kwon SK, Lee SH, Kitada T, Kim JM, Chung J. PINK1 controls mitochondrial localization of Parkin through direct phosphorylation. Biochem Biophys Res Commun. 2008 Dec 19;377(3):975-80.

Krige D, Carroll MT, Cooper JM, Marsden CD, Schapira AH. Platelet mitochondrial function in Parkinson's disease. The Royal Kings and Queens Parkinson Disease Research Group. Ann Neurol. 1992 Dec;32(6):782-8.

Kuroda Y, Mitsui T, Kunishige M, Matsumoto T. Parkin affects mitochondrial function and apoptosis in neuronal and myogenic cells. Biochem Biophys Res Commun. 2006 Sep 29;348(3):787-93.

Kushnareva Y, Murphy AN, Andreyev A. Complex I-mediated reactive oxygen species generation: modulation by cytochrome c and NAD(P)+ oxidation-reduction state. Biochem J. 2002 Dec 1;368(Pt 2):545-53.

Larsen NJ, Ambrosi G, Mullett SJ, Berman SB, Hinkle DA. DJ-1 knock-down impairs astrocyte mitochondrial function. Neuroscience. 2011 Nov 24;196:251-64.

Lee EJ, In KH, Kim JH, Lee SY, Shin C, Shim JJ, Kang KH, Yoo SH, Kim CH, Kim HK, Lee SH, Uhm CS. Proteomic analysis in lung tissue of smokers and COPD patients. Chest. 2009 Feb;135(2):344-52.

Lees AJ, Hardy J, Revesz T. Parkinson's disease. Lancet. 2009 Jun 13;373(9680):2055-66.

Lev N, Ickowicz D, Melamed E, Offen D. Oxidative insults induce DJ-1 upregulation and redistribution: implications for neuroprotection. Neurotoxicology. 2008 May;29(3):397-405.

Li HM, Niki T, Taira T, Iguchi-Ariga SM, Ariga H. Association of DJ-1 with chaperones and enhanced association and colocalization with mitochondrial Hsp70 by oxidative stress. Free Radic Res. 2005 Oct;39(10):1091-9.

Lin TK, Liou CW, Chen SD, Chuang YC, Tiao MM, Wang PW, Chen JB, Chuang JH. Mitochondrial dysfunction and biogenesis in the pathogenesis of Parkinson's disease. Chang Gung Med J. 2009 Nov-Dec;32(6):589-99.

Navarro A, Boveris A. Brain mitochondrial dysfunction and oxidative damage in Parkinson's disease. J Bioenerg Biomembr. 2009 Dec;41(6):517-21.

Nicholls DG, Budd SL. Mitochondria and neuronal survival. Physiol Rev. 2000 Jan;80(1):315-60.

Nguyen T, Nioi P, Pickett CB. The Nrf2-antioxidant response element signaling pathway and its activation by oxidative stress. J Biol Chem. 2009 May 15;284(20):13291-5.

Penn AM, Roberts T, Hodder J, Allen PS, Zhu G, Martin WR. Generalized mitochondrial dysfunction in Parkinson's disease detected by magnetic resonance spectroscopy of muscle. Neurology. 1995 Nov;45(11):2097-9.

Plun-Favreau H, Hardy J. PINK1 in mitochondrial function. Proc Natl Acad Sci US A. 2008 Aug 12;105(32):11041-2.

Plun-Favreau H, Klupsch K, Moisoi N, Gandhi S, Kjaer S, Frith D, Harvey K, Deas E, Harvey RJ, McDonald N, Wood NW, Martins LM, Downward J. The mitochondrial protease HtrA2 is regulated by Parkinson's disease-associated kinase PINK1. Nat Cell Biol. 2007 Nov;9(11):1243-52.

Poole AC, Thomas RE, Andrews LA, McBride HM, Whitworth AJ, Pallanck LJ. The PINK1/Parkin pathway regulates mitochondrial morphology. Proc Natl Acad Sci U S A. 2008 Feb 5;105(5):1638-43.

Pridgeon JW, Olzmann JA, Chin LS, Li L. PINK1 protects against oxidative stress by phosphorylating mitochondrial chaperone TRAP1. PLoS Biol. 2007 Jul;5(7):e172.

Purves D, Augustine GJ, Fitzpatrick D, et al., editors. Neuroscience. 3rd edition. Chapter 1: Studying the Nervous Systems of Humans and Other Animals. Sunderland (MA): Sinauer Associates; 2004.

Repetto G, del Peso A, Zurita JL. Neutral red uptake assay for the estimation of cell viability/cytotoxicity. Nat Protoc. 2008;3(7):1125-31.

Riss TL, Moravec RA, Niles AL, Benink HA, Worzella TJ, Minor L. Cell Viability Assays. 2013 May 1 [updated 2015 Jun 29]. In: Sittampalam GS, Coussens NP, Nelson H, Arkin M, Auld D, Austin C, Bejcek B, Glicksman M, Inglese J, Iversen PW, Li Z, McGee J, McManus O, Minor L, Napper A, Peltier JM, Riss T, Trask OJ Jr., Weidner J, editors. Assay Guidance Manual [Internet]. Bethesda (MD): Eli Lilly & Company and the National Center for Advancing Translational Sciences; 2004.

Schapira AH, Cooper JM, Dexter D, Clark JB, Jenner P, Marsden CD. Mitochondrial complex I deficiency in Parkinson's disease. J Neurochem. 1990 Mar;54(3):823-7.

Sherer TB, Betarbet R, Testa CM, Seo BB, Richardson JR, Kim JH, Miller GW, Yagi T, Matsuno-Yagi A, Greenamyre JT. Mechanism of toxicity in rotenone models of Parkinson's disease. J Neurosci. 2003 Nov 26;23(34):10756-64.

Sherer TB, Betarbet R, Kim JH, Greenamyre JT. Selective microglial activation in the rat rotenone model of Parkinson's disease. Neurosci Lett. 2003 May 1;341(2):87-90.

Sherer TB, Richardson JR, Testa CM, Seo BB, Panov AV, Yagi T, Matsuno-Yagi A, Miller GW, Greenamyre JT. Mechanism of toxicity of pesticides acting at complex I: relevance to environmental etiologies of Parkinson's disease. J Neurochem. 2007 Mar;100(6):1469-79.

Shimura H, Mizuno Y, Hattori N. Parkin and Parkinson disease. Clin Chem. 2012 Aug;58(8):1260-1.

Silvestri L, Caputo V, Bellacchio E, Atorino L, Dallapiccola B, Valente EM, Casari G. Mitochondrial import and enzymatic activity of PINK1 mutants associated to recessive parkinsonism. Hum Mol Genet. 2005 Nov 15;14(22):3477-92.

Song YJ, Halliday GM, Holton JL, Lashley T, O'Sullivan SS, McCann H, Lees AJ, Ozawa T, Williams DR, Lockhart PJ, Revesz TR. Degeneration in different parkinsonian syndromes relates to astrocyte type and astrocyte protein expression. J Neuropathol Exp Neurol. 2009 Oct;68(10):1073-83.

Taira T, Saito Y, Niki T, Iguchi-Ariga SM, Takahashi K, Ariga H. DJ-1 has a role in antioxidative stress to prevent cell death. EMBO Rep. 2004 Feb;5(2):213-8.

Testa CM, Sherer TB, Greenamyre JT. Rotenone induces oxidative stress and dopaminergic neuron damage in organotypic substantia nigra cultures. Brain Res Mol Brain Res. 2005 Mar 24; 134(1):109-18.

Trempe JF, Fon EA. Structure and Function of Parkin, PINK1, and DJ-1, the Three Musketeers of Neuroprotection. Front Neurol. 2013 Apr 19;4:38.

Tufekci KU, Civi Bayin E, Genc S, Genc K. The Nrf2/ARE Pathway: A Promising Target to Counteract Mitochondrial Dysfunction in Parkinson's Disease. Parkinsons Dis. 2011 Feb 22;2011:314082.

Van Laar VS, Berman SB. Mitochondrial dynamics in Parkinson's disease. Exp Neurol. 2009 Aug;218(2):247-56.

Wilson MA. The role of cysteine oxidation in DJ-1 function and dysfunction. Antioxid Redox Signal. 2011 Jul 1;15(1):111-22.

Whittemore ER, Loo DT, Watt JA, Cotman CW. A detailed analysis of hydrogen peroxide-induced cell death in primary neuronal culture. Neuroscience. 1995 Aug;67(4):921-32.

Yanagida T, Tsushima J, Kitamura Y, Yanagisawa D, Takata K, Shibaike T, Yamamoto A, Taniguchi T, Yasui H, Taira T, Morikawa S, Inubushi T, Tooyama I, Ariga H. Oxidative stress induction of DJ-1 protein in reactive astrocytes scavenges free radicals and reduces cell injury. Oxid Med Cell Longev. 2009 Jan-Mar;2(1):36-42.

Zhang L, Shimoji M, Thomas B, Moore DJ, Yu SW, Marupudi NI, Torp R, Torgner IA, Ottersen OP, Dawson TM, Dawson VL. Mitochondrial localization of the Parkinson's disease related protein DJ-1: implications for pathogenesis. Hum Mol Genet. 2005 Jul 15;14(14):2063-73.

Zhong N, Kim CY, Rizzu P, Geula C, Porter DR, Pothos EN, Squitieri F, Heutink P, Xu J. DJ-1 transcriptionally up-regulates the human tyrosine hydroxylase by inhibiting the sumoylation of pyrimidine tract-binding protein-associated splicing factor. J Biol Chem. 2006 Jul 28;281(30):20940-8.